HAWASSA UNIVERSITY

COLLEGE OF NATURAL AND COMPUTATIONAL SCIENCE

SCHOOL OF POST GRAGUATE STUDIES

DEPARTEMENT OF CHEMISTRY

M.Sc. THESIS

PREPARATION OF BIOSORBENTS FROM *JATROPHA CURCAS* LEAF FOR THE REMOVAL OF MALCHITE GREEN FROM AQUEOUS SOLUTION

BY:

AYUB HAJI

ADVISOR: ERMIYES HAILE (ASS. PROFESSOR)

OCTOBER, 2024

HAWASSA, ETHIOPIA

PREPARATION OF BIOSORBENTS FROM *JATROPHA CURCAS* LEAF FOR THE REMOVAL OF MALCHITE GREEN FROM AQUEOUS SOLUTION

A THESIS SUBMITTED TO SCHOOL OF GRADUATE STUDIES, HAWASSA UNIVERSITY IN PARTIAL FULFILLMENT OF THE REQUIREMENTS FOR THE DEGREE OF MASTER OF SCIENCE IN CHEMISTR

BY:

AYUB HAJI

ADVISOR: ERMIYES HAILE (ASS. PROFESSOR)

OCTOBER, 2024

HAWASSA, ETHIOPIA

DECLARATION

This thesis is my original work except where due reference has been made properly acknowledged. This work has not been submitted for MSc degree in any other university

Name of student: Ayub Haji Burka

Signature: _____

Date:_____

This thesis has been submitted for examination with my approval as a university advisor.

Name of Advisor: Ermiyes Haile (Ass. professor)

Signature: _____

SCHOOL OF GRADUATE STUDIES

HAWASSA UNIVERSITY

APPROVAL SHEET-1

This is to certify that the thesis entitled **"Preparation of biosorbents from *Jatropha curcas* leaf for the removal of malachite green from aqueous solution**" submitted in partial fulfillment of the requirements for the degree Master of Science in Chemistry, in the graduate program of the Department of Chemistry which has been conducted by **Ayub Haji (ID PGCHEMK 005/10**) Were done under my supervision. Therefore, we recommend that the student has fulfilled the requirements and hence hereby can submit the thesis to the department.

Ermiyes Haile (Ass. Prof.)

_____	_____	_____
Name of advisor	Signature	Date

SCHOOL OF GRADUATE STUDIES

HAWASSA UNIVERSITY

APPROVAL SHEET-2

We, the undersigned, members of the board of Examiners of the final defense by Ayub Haji read and evaluated this thesis entitled "**Preparation of biosorbents from *Jatropha curcas* leaf for the removal of malachite green from aqueous solution**" "examined the candidate. This is, therefore to certify that, the thesis has been accepted partial fulfillment of the requirements for the degree of masters of Science in chemistry.

Name of Chairperson	Signature	Date
Name of internal examiner	Signature	Date
Name of external examiner	Signature	Date
Name of advisor	Signature	Date
SGS/DGC	Signature	Date

ACKNOWLEDGMENT

I would like to extend my gratitude to all those who have made immense contribution to the success of this research and also made my M.Sc. journey worthwhile. Top on my long list is my advisor Ermiyes Haile (Assistant Professor) for his guidance and dedication towards the successful completion of this thesis. It has been a great pleasure and honor to my advisor and I cannot thank him enough for the knowledge and experience that I have acquired working with him.

I would like to extend my gratitude to the all the laboratory technicians, staff and my colleagues at Hawassa University, College of Natural and Computational Sciences, Department of Chemistry. Next, I would like to thanks to Mr. Leta (M. Sc.) for his unreserved support during SEM analysis at Adama Science and Technology University.

I give special thanks to my family, and in laws, thank you all for the love and encouragement that helped me persevere during challenging times in my research. And to my wonderful friends and colleagues here in the Hawassa University and all over, I can neither repay the assistance that I have received over the past few years nor able to fit in the names of everyone into this small page. I say a big thank you all and God bless.

TABLE OF CONTENTS

LIST OF TABLES

LIST OF FIGURES

LIST OF SYMBOL AND ABBREVIATIONS

FT-IR	Fourier Transforms Infrared Spectroscopy
MG	Malachite Green
PFO	Pseudo first order
ppb	Part per Billion
Ppm	Part per Million
PSO	Pseudo second order
qe	The Amount of Adsorbate per Gram Adsorbent at Equilibrium ($mg.g^{-1}$)
qm	Equilibrium Adsorption Capacity Using Model
qmax	Maximum Adsorption Capacity (mg/g)
qt	The Amount of Adsorbate per Gram of Adsorbent at Any Time
SEM	Scanning Electron Microscope
t	Time (min)
T	Temperature (K)
Uv/vis	Ultraviolet Visible

ABSTRACT

Malachite green used in textile and dyeing industries is a common persistent pollutant in wastewater and the environment causing major hazards to human health and aquatic organisms. The main objective of the study was to prepare biosorbent from Jatropha curcas leaf for the removal of malachite green from aqueous solution. Biosorbent was prepared from Jatropha curcas leaf using chemical activation method. Characterization techniques including FTIR and SEM analysis of biosorbent was evaluated. The FTIR analysis showed the presence of phenols, aromatic compound, lignin, ketone and aldehyde on biosorbent surface and after adsorption spectra revealed the great interaction of malachite green with the surface functional group of biosorbent. SEM analysis revealed that biosorbent was irregular, porous and heterogeneous, and after adsorption shows that great affinity of malachite green on the surface of biosorbent. The removal percentage and adsorption capacities of malachite green from aqueous solution was 99.6% and 49.8 mg/g was obtained at optimal condition of pH 8, 10 mg/L of initial concentration, 0.2 g/L of adsorbent dosage, 90 minutes of contact time and 45 ℃. Freundlich model was best fit for removal of malachite green from aqueous solution than Langmuir due to its higher correlation coefficients and lower mean standard error (MSE) (R^2: 0.99993, MSE:0.000055). Pseudo second order was well fitted for the adsorption of malachite green from aqueous solution than pseudo first order due to its higher coefficients and lower sum square error (SSE) (R^2:0.99999, SSE: 0.000051). Thermodynamic analysis presented that the adsorption process of malachite green from aqueous solution was employed spontaneous process and endothermic reaction. These findings suggest that the use of biosorbent prepared from Jatropha curcus was cost-effective for the removal of malachite green from contaminated environment.

Keywords: Biosorbent, Malachite Green, Adsorption, *Jatropha curcas* and environmentally friendly

1. INTRODUCTION

1.1. Background of the study

Water pollution caused by wastewater from textile manufacturing activities is a major global concern. One of the most difficult tasks that researchers are faced with around the world in the twenty-first century is to provide the clean water necessary for industrial, house hold, and agricultural activities [1]. Textile factories are responsible for one of the major environmental pollution issues in the world, because they discharge undesirable dye effluents [2]. The textile industry consumes 100–200 L of water per kg of textiles produced, resulting in the generation of large amounts of wastewater during the dyeing process [3]. Globally, about 280,000 tons of synthetic dyes are discharged into natural streams every year from wastewater produced by variety industries, such as leather, food, textile, paper, cosmetic, printing, and carpet manufacturers [4]. The said discharge has an adverse impact on the visual quality of water bodies, and it interferes with the lifecycles of aquatic organisms by reducing the penetration of sunlight into the water, which inhibits photosynthesis and plant growth, thereby affecting the biological activity of aquatic animals; moreover, the synthetic dyes present in water bodies also cause soil contamination [5].

Malachite green (MG) is a synthetic dye used to dye silk, cotton, leather, wool, and paper, and it is also employed as a fungicide and disinfectant in the fish farming industry, as it affords the control of fish parasites and diseases [6]. MG is a cationic triphenylmethane compound that is highly soluble in water [7]. It is also highly toxic to mammalian cells at concentrations below 0.1 g/mL [8]. MG is characterized by a complex molecular structure, high stability, non-biodegradability, and high resistance to light and oxidizing agents [7]. When it flows into the receiving stream, this dye negatively affects the lifecycles of aquatic organisms by interfering with the physiology of the pituitary liver, gills, kidneys, intestines, gonads, and gonad vegetative cells [9]. In humans, MG inhalation can cause inflammation of the respiratory tract, while its swallowing can cause inflammation of the digestive tract [10]. MG is hazardous to humans, and mutagenic; additionally, its presence affects the immunological and reproductive systems [11]. Malachite green can be converted into leuco Malachite green and carbinol, which is toxic to humans. In fish muscles, fat, and internal organs, MG has a half-life of 10 days [12]. This

cationic dye is also durable in the environment, with a half-life of 12.9–50.34 days in sediment [13].

Various methods have been used to treat textile wastewater, including physical, chemical, and advanced treatment methods, such as membrane filtration, ion exchange, electrochemical technology, coagulation, flocculation, reverse osmosis, chemical oxidation, ozonation [14], and biological treatment for fungi and bacteria effects [15]. However, most of these methods have various disadvantages, including low efficiency, large capital investment, high energy consumption, high cost, non-selectiveness, unsuitability for large-scale applications, and the formation of harmful secondary sludge [16]. Among the treatment strategies, adsorption is one of the most appealing and efficient methods for removing dyes from polluted water samples. This technique provides various advantages, including a simple design, recyclable adsorbents, simple operation, non-toxicity, low cost, and a modest initial investment [17].

Some of the organic ingredients such as mangosteen rind, algae, water hyacinth and oil palm have previously been used as biosorbent. These natural adsorbents are able to absorb organic pollutant from the environment efficiently in their role as biosorbents and dye bioaccumulation. The presence of secondary metabolites such as flavonoids with amino groups, carboxyl, thiol, hydroxyl-carbonyl and phosphate was form complex compounds with malachite green [18-19]. Biosorbents are made from all natural materials that contain carbon, both organic carbon and inorganic carbon with the condition that the material has a porous structure, like *Jatropha curcas* leaves [20]. *Jatropha curcas* leaves have relatively large porous structure and contain some of organics group which induce as a function of biosorbents for the development of water purification contaminated with malachite green [19]. While unmodified *Jatropha curcas* leaf was less effective comparable to modified biosorbents for the removal of organic pollutant from wastewater. In chemical activation the precursor is impregnated with an activating agent such as, H_3PO_4, H_2SO_4 and NaOH used for modification of biosorbents [21]. Modified biosorbents effective for the removal of organic pollutant from aqueous solution due to its high porosity and surface area, enhance adsorption capacity and good development of the porous structure [22].

1.2. Statement of the Problem

In developing countries the developments of industrialization affect the source of water quality. The discharge of industrial waste including textile and lather into water bodies causes water pollution due to high accumulation of organic and inorganic pollutant [23]. Malachite green (MG) dye has been widely used for the dyeing of leather, wool, jute and silk, as in distilleries, as a fungicide and antiseptic in aquaculture industry to control fish parasites and disease [23]. However, excessive malachite green solution in water bodies has negative effect on the growth of aquatic plants and algae [24]. This could lead to a variety of water quality problems including low dissolved oxygen concentrations, reduced species of fish, harm other aquatic life and indirectly affect human health by causes damage to the liver, spleen, kidney and heart; inflicts lesions on the skin, eyes, lungs and bones; and produces teratogenic effects and highly cytotoxic to mammalian cells [25]. Then adsorption is the most effective method with biosorbent for the removal of accumulation of malachite green from aqueous solution due to its stability, high surface area and porosity, cost effective and environmental friendly. Biosorbent was prepared from *Jatropha curcas* leaves using chemical activation method. In Ethiopia *Jatropha curcas leaf* was agricultural waste and conversion of *Jatropha curcas* leaves into value added product has multidimensional purpose used as waste management and environmental sustainability. *Jatropha Curcas* leaves biosorbents was efficiently remove malachite green from aqueous solution. Therefore no literature data was reported on the preparation of biosorbent from *Jatropha Curcas* leaves for the removal of malachite green from aqueous solution.

1.3. Objective of the study

1.3.1. General objective

- To investigate preparation of biosorbents from Jatropha curcas leaf and its removal capacity of malachite green from aqueous solution.

1.3.2. Specific Objectives

- ✓ To prepare biosorbents from *Jatropha curcas* leaf by chemical activation using H_3PO_4, NaOH and H_2SO_4.
- ✓ To determine chemical composition and surface morphology of biosorbent using FTIR and SEM method.

- ✓ To evaluate the effect of pH, adsorbent dosage, initial concentration and contact time for the removal of malachite green from aqueous solution.
- ✓ To study the potential effect of biosorbent for the removal of malachite green from aqueous solution.
- ✓ To assess the effect of thermodynamic process for the removal of malachite green from aqueous solution.

1.4. Research question

The research of the study tried to address the following significant questions;

1. What is the preparation method of biosorbent from biomass?
2. What is the chemical composition and surface morphology of biosorbent?
3. What is the effect of pH, adsorbent dosage, initial concentration and contact time for the removal of malachite green from aqueous solution?
4. What if the potential effect of biosorbent for the removal of malachite green from aqueous solution?
5. What is the effect of thermodynamic process for the removal of malachite green from aqueous solution?

1.5. Significance of the study

This study gives information about removal of malachite green from wastewater by biosorbents prepared from *Jatropha Curcas* leaves to stakeholders including water resource and irrigation management and concerned body. The prepared biosorbents was good biosorbent for organic and inorganic pollutant from water sample. The finding of the study is used as references for further researcher to study with related schematic area.

1.6. Scope of the study

This study was focus on the preparation of *Jatropha curcas* leaf for the removal of malachite green from aqueous solution. Therefore, biosorbents preparation, chemical composition, surface morphology and optimization parameters, adsorption experiment, adsorption model, kinetic model analysis and thermodynamic study were conducted in this study.

2. LITIRETURE REVIEW

2.1. Chemistry of Dye

Dyes are colored compounds which are widely used in textiles, printing, rubber, cosmetics, plastics, leather industries to color their products results in generating a large amount of colored wastewater [26]. Mainly dyes are classified into anionic, cationic, and non-ionic dyes. Among all the dyes using in industries, textile industries placed in the first position in using of dyes for coloration of fiber. In addition, an understanding of color and constitution relationships has always been of critical importance in the design of new dyes, perhaps the most notable early contribution to the science of the color referred to as the chromophores and auxochromes [27]. The chromophores and auxochromes theory is proposed as a simple method for explaining the origin of color in dye molecules, although it lacks rigorous theoretical justification. The most important chromophores, as defined in this way are the carbonyl(C=O), diazo(-N=N-), azomethine(-CH=N) and nitro(NO_2) group. Other groups increase the intensity of the color and shift the absorption to longer wave length of light, including hydroxyl ($O\overline{H}$) and amino (NR_2) [28].

Dyes are mainly derived from natural sources without any chemical treatment such as plants, insects, animals and minerals. Dyes derived from plant sources are indigo and saffron, insects are cochineal beetles and lac scale insects, animal sources are derived from some species of mollusks or shellfish, and minerals are ferrous sulfate, ochre. Industries such as textile, printing, paper, carpet, plastic, and leather use dyes to provide color to their products. These dyes are always left in industrial waste and consequently discharged into the water body [29-30].

Dyes release into waste water from various industrial outlets, such as paper, food coloring, cosmetics, leather, pharmaceutical, dyeing, printing, carpet industries etc. The textile manufacturing and dyeing industries utilize more quantities of a large number of dyes and release these dye pollutants into environment as waste water effluents. These dyes are highly toxic and even carcinogenic to microbial populations and mammalian animals hence these are needed to remove from the water effluents before they are released into water bodies. Dyes are stable to light and not biologically degradable; they are resistant to aerobic digestion and signify one of the difficult groups to be removed from the industrial wastewater [31-33].

2.2. Classification of dyes

There are two methods used to classify dyes, either according to their chemical structure (particularly considering the chromophoric structure present in the dye molecule) or according to how it is applied to the substrate (Figure 1). The first method is adopted by practicing dye chemists and includes azo, anthraquinone, etc. dyes. The latter method was adopted by the colour index [34].

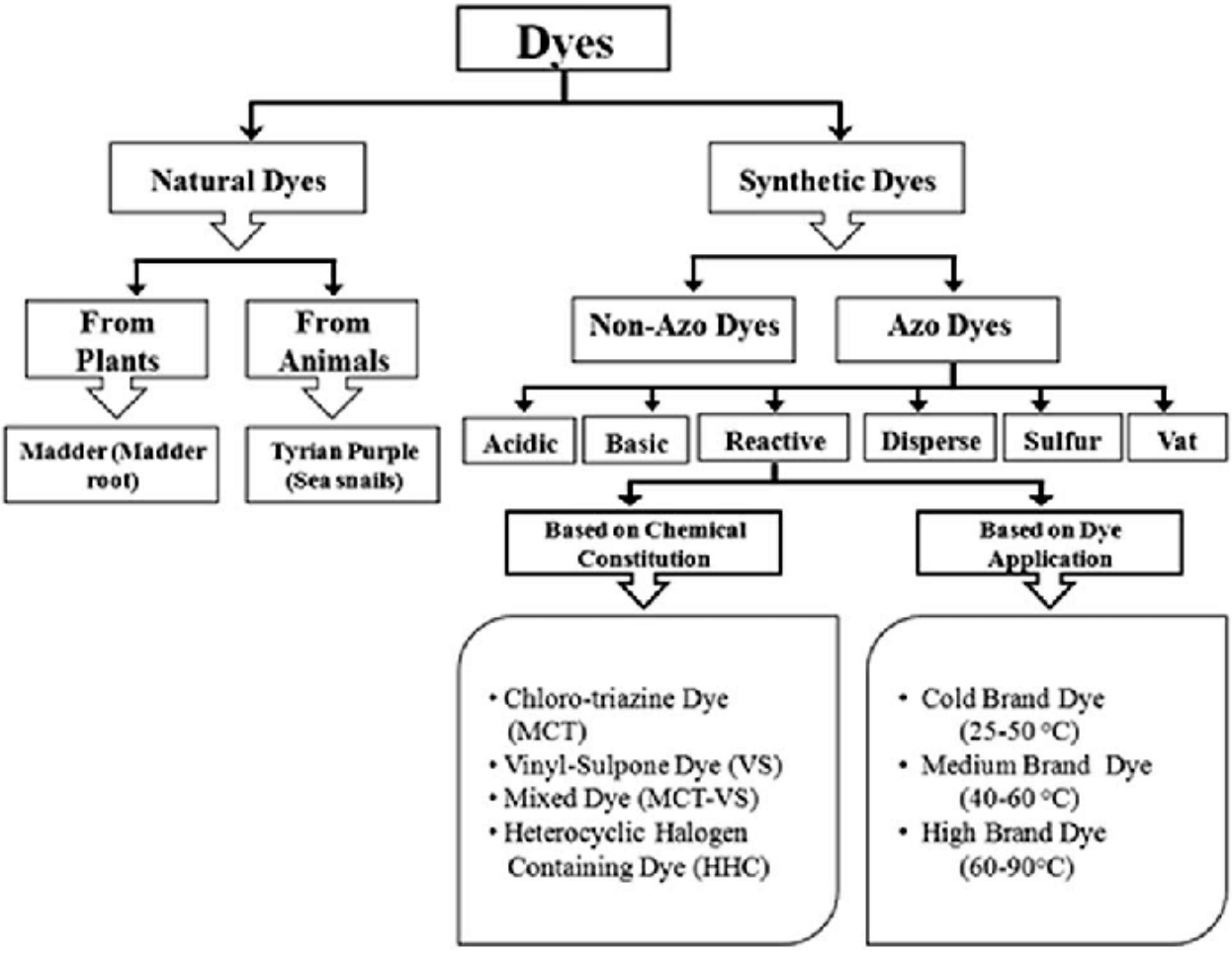

Figure 1: Classification of dyes

2.2. Physicochemical properties of Malachite Green

Malachite green (MG) is water soluble cationic dye that appears as green crystalline powder and belongs to triphenylmethane category [35]. Malachite green oxalate is [4-[[4-(Dimethylamino) phenyl]-phenyl methylidene] cyclohexa-2, 5-dien-1-ylidene]-dimethyl azanium; 2-hydroxy-2-oxoacetate; oxalic acid and has a chemical formula of $C_{52}H_{54}N_4O_{12}$ with molecular weight of

927.00 g/mol. The chemical structure of MG dye is presented in Figure 2 below. . Its crystalline form appears as a dark green color, which transforms into a blue hue upon dissolution in water [35, 23, 24]. MG exhibits a pKa value ranging from 3.70 to 4.80 and demonstrates monoprotic Bronsted acid-base characteristics [9]. Within the textile industry, MG finds application in the dyeing of leather, wool, and silk. It possesses advantageous properties, such as antibacterial, antifungal, and antiparasitic effects, which are beneficial for aquaculture. Furthermore, it is a cost-effective dye that enjoys global availability.

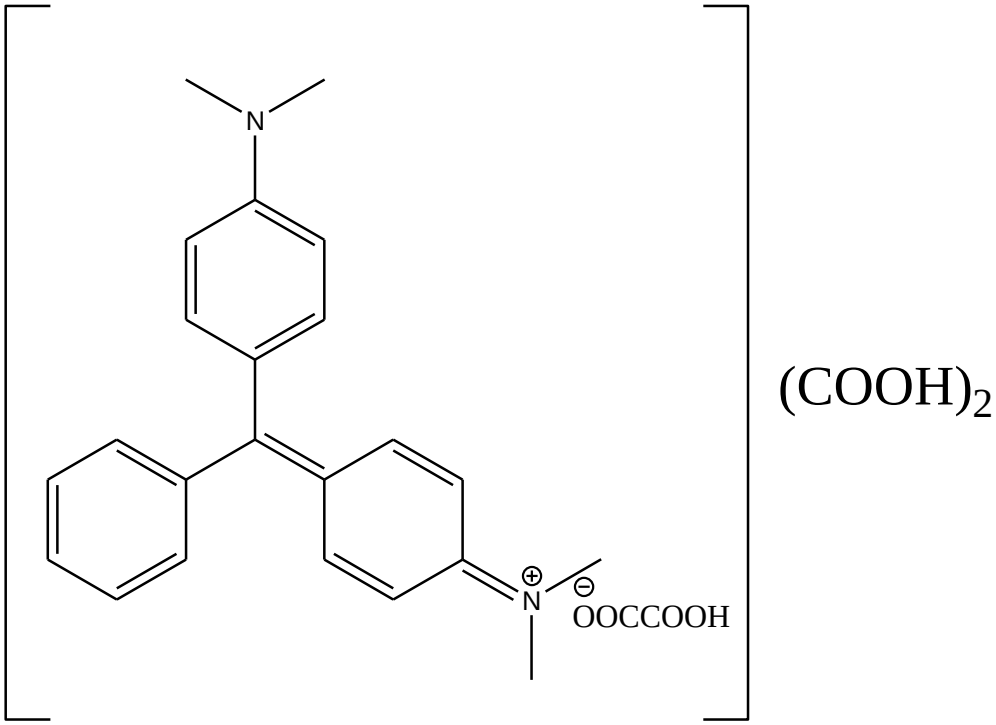

Figure 2: Chemical structure of malachite green

2.3.Environmental Pollution of Dyes

Any industrial activities causes pollution in one form or the other so is the textile industry. Wastewater is the most environmentally damaging, and the wastewater from textile plants is classified as the most polluting of all the industrial sectors, considering the volume generated as well as its composition. The dyestuff lost through the processes of the textile poses a major problem for wastewater treatment [34].

Through the dyeing process, depending on the class of the dye, its loss in wastewaters could vary from 2% for basic dyes to as high as 50% for reactive dyes, leading to severe contamination of surface and ground waters. Color is the first wastewater contaminant to be recognized, since a very small amount of dye concentration in water (<1ppm) are highly visible that affects aesthetic merit, transparency and water-gas solubility. Moreover reducing light penetration through water decreases photosynthetic activity, generating oxygen deficiency and de-regulating the biological cycles of aquatic biota [36]. Many dyes are also highly toxic to the ecosystem and mutagens, meaning they can have acute to chronic effects upon organisms, depending on exposure time and dye concentration. For example, dye effluent has been connected to growth reduction, metabolic stress and death in fish, and growth and productivity in plants. Contamination therefore limits downstream human water use such as recreation, drinking, fishing and irrigation [37]. Therefore, wastewater containing residual dyes need to be treated before discharging to the receiving environment to keep the environment eco-friendly and sustainable.

Continuous urbanization and the growth of industrialization have disturbed the balance of environmental composition through the release of hazardous materials, smoke, and noxious gases which consequently lead to toxic effects on living things [38]. As shown in (Figure 3). Environmental pollution, especially water pollution is a critical problem in the world. Organic dyes and their effluents are one of the main sources of water pollution which are commonly escaped from the wastewater treatment plants including the mining, textile, paper printing, food processing, cosmetics, pharmaceutical, and leather industries [39]. Contaminated water occurs when unwanted contaminants enter bodies of water or lakes, rendering them unfit for drinking and other uses [40]. Currently, under present circumstances, sustaining a pure and healthy air and water environment is a key challenge [41]. Fortunately, novel technologies are now in practice to remediate undesirable products from the air, water, and soil. Among them, nanotechnology exhibits great potential to build and use novel and cost-effective techniques for the monitoring of contaminants, degradation via catalysis, adsorptive removal, and cleaning of environmental pollution [42].

Figure 3: Discharging of dye into environment

2.4. Wastewater Treatment method

Wastewater discharged from industries contain contaminates including dyes. Removal of dyes from industrial wastes using different methods has been needed. Dyes are mainly engaged in the textile, food, pharmaceutical, cosmetics, and plastics, photographic and paper industries. Though the rapid industrialization is the best way to achieve economic growth, it affects human health directly or indirectly by escaping wastes into water bodies. Environmental legislation obliges industries to eliminate color for their dye containing effluents before disposal into the water. The technologies used for the removal of dye can be categorized into: biological, chemical and physical methods [43].

2.4.1. Biological Methods

Biological treatments often the most economical alternative when compared with other physical and chemical processes. Methods like fungal decolorization, microbial decolorization, adsorption by(living or dead) microbial biomass and bioremediation systems are commonly applied to the treatment of industrial emission because many microorganisms such as bacteria, yeast, algae and fungi are able to accumulate and degrade different dyes[Fu &Viraraghavan,2001]. But biological treatment requires large area and this method is unsatisfactory in color elimination with current biodegradation processes [44].

2.4.2. Chemical methods

Chemical methods include coagulation or flocculation combined with floatation and filtration, precipitation, electro floatation, electro kinetic coagulation, conventional oxidation methods by oxidizing agents such as ozone, irradiation or electrochemical processes. Though the dyes are removed completely by this process, it is so expensive and also accumulation of concentrated sludge creates a disposal problem. Expensive chemical uses generates secondary pollution problem [45].

2.4.2.1.Electrocoagulation

This method is widely used to decolorize dyes. It is straight forward and proficient method for the treatment of waste comprising dyes. In recent years, many investigations have been specially focused on the use of electrocoagulation owing to increase in environmental restrictions on effluents wastewater. Electrocoagulation is a process consisting of creating metallic hydroxide flocks inside the wastewater by electro dissolution of soluble anode made of iron or aluminum [46].

2.4.2.2.Electrochemical oxidation

This method is used as an alternative treatment process for the removal of color in dye solution. Electrochemical oxidation is capable of destroying the chromophores groups, and full decolorization of dyes found in textile effluents can be done at short treatment times. Indirect electrochemical oxidation via hydroxyl radicals convenient way for the degradation and mineralization of reactive dyes and offers approach to developing new technology for removal of reactive dyes in real textile industry effluents with low energy consumption [47].

2.4.2.3.Photochemical degradation

Photo chemical catalysis is one of the advanced oxidation processes, is a new method used to mineralized dye compounds. One of the major advantages of the photo catalytic degradation over existing technologies is that there is no further requirement for secondary disposal methods [48].

2.4.3. Physical methods

Physical methods used commonly are membrane filtration processes (Nano filtration, reverse osmosis, electro dialysis) and adsorption technique [49].

2.5. Chemical activation of Biosorbent

The preparation with different pore sizes can be achieved by physical or chemical activation process. In both methods, the development of porosity is different in terms of practical procedures and mechanism. In physical activation, the generation of porosity took place via selective elimination of the more reactive carbon of the structure and further gasification led to the production of the bio-sorbent with high porosity. In chemical activation process, the precursor is mixed with a chemical such as sulphate salts, chloride salts, NaOH, $CaCl_2$, H_2SO_4, H_3PO_4 and washed to produce the activated biosorbents, Following the thermal decomposition of the precursor, the chemical reacts with the product causing reduction in the evolution of volatile matter and inhibition of the particle shrinkage. Once the chemical is removed by exhaustive washing, a large amount of porosity is formed [50]. The activations of lingo cellulosic materials with H_3PO_4 has become an increasingly used method for the large-scale manufacture of biosorbent (Figure 4) because the use of this reagent has some environmental advantages such as ease of recovery, low energy cost and high carbon yield. H_3PO_4 plays two roles during the preparation of biosorbent: H_3PO_4 acts as an acid catalyst to promote bond cleavage, hydrolysis, dehydration and condensation, accompanied by cross-linking reactions between phosphoric acid and biopolymers; H_3PO_4 may function as a template because the volume occupied by phosphoric acid in the interior of the activated precursor is coincident with the micro pore volume of the bio-sorbent obtained [51].

Figure 4: Effect of chemical activation on the surface of biosorbent

2.6.Adsorption

Adsorption using different adsorbent is superior to the other separation techniques because of its efficacy, economy, ability to separate a wide range of chemical compounds and simple procedure. It the process in which different molecules, ions and atoms of liquid or gas gets attached to surface of the solid. Adsorbate is attached in the form of a film on the surface of the adsorbent. This process is different from absorption since in absorption, the substrate, which is usually in the form of fluid, percolates into the absorbent [51]. Thus, absorption includes the whole matter whereas adsorption is only effective on surfaces. However, both terms are include in a single term called sorption and the reverse is called desorption. Thus, in the process of

adsorption, the substance is separated from fluid phase and is accumulated on the solid phase substrate.

Adsorption offers significant advantages like low cost, availability, profitability, ease of operation and efficiency in comparison with the conventional methods especially from economic and environmental point of view. It involves movement of substance from liquid phase to solid phase. The transferred substance is bound by chemical or physical interactions [52]. Adsorption mainly is used in purification of gases or liquid. The adsorbing material is known as adsorbent. The material being adsorbed is called adsorbate. The interaction between the two is characterized by strong covalent or ionic bond. The chemical adsorption is also called chemisorption while physical adsorption is also called physisorption [53].

2.7.Effect of Biosorbent for the Removal of Malachite green

Abewaa *et al*. [54] reported that The maximum and minimum malachite green removal efficiencies of 99.9% and 62.4% were observed at their respective experimental conditions of (100 mg/L, 0.10 mg/100 mL, pH 6, and 40 min) and (100 mg/L, 0.15 mg/100 mL, pH 3, and 20 min), respectively on the surface of *Rumex abyssinicus* derived activated carbon. Wood apple shell, a fruit-food solid waste, was successfully utilized as a low cost alternative adsorbent for the removal of hazardous dye MG. The removal of MG dye was found to be 98.87% with initial concentration 100 mg/L at pH 7–9 in 3.30 h by shaking at 150 rpm at 299 ± 2 K [23]. According to Gietu *et al*. [24] literature report the adsorption performance of the prepared activated carbon from *Catha edulis* stem was optimized by varying operational parameters such as initial dye concentration (10 mg/L), pH (10), dosage (0.5 g), and contact time (60 min). The maximum removal efficiency of the prepared adsorbent at those optimum conditions was 98.8%.

The removal of MG from aqueous solution revealed that the process was influenced by initial concentration, pH and temperature of dye solution as well as teak leaf litter dosage. Optimum uptake of the dye per gram of the adsorbent occurred at 2 g/L and at pH 6-10. Dubinin–Radushkevich and Freundlich isotherm models fit the batch adsorption data better than Langmuir isotherm. However, the monolayer capacity of teak leaf litter for the removal of MG in aqueous solution was calculated to be 333.33 mg/g at 293-313 K [55].

As Moumni *et al*. [56] reported that the removal capacity of malachite green from aqueous solution was 2.66 mg/g and 23.48 mg/g on the surface of byproduct of lightweight composite bricks adsorbent obtained at 20 mg/L initial concentration, adsorbent dose of 0.15 g/mL, a pH of 10, and an adsorption time of 180 minutes. While the thermodynamic study conducted at four temperatures (298 K, 308 K, 318 K, 328 K) revealed that the adsorption process is spontaneous and endothermic in nature.

2.8.Mechanism of Adsorption

Adsorption occurs when the adsorbate and adsorbent surfaces reach equilibrium. This equilibrium is achieved through a series of steps known as the adsorption mechanism. The adsorption mechanism for dye onto its adsorbent typically involves four stages: (1) the transfer of the dye solution to the bulk adsorbent surface; (2) diffusion of the dye through the boundary layer to the adsorbent surface; (3) movement of the dye from the adsorbent surface to the interior pores; (4) adsorption occurring at the active sites of the adsorbent surface [57]. For cationic dyes like malachite green, the adsorption mechanisms may involve various processes such as electrostatic attraction, formation of hydrogen bonds, pore filling, n-π interactions, and π-π interactions (Figure 5) [58].

These mechanisms contribute to the overall adsorption of the dye onto the adsorbent surface. The adsorption mechanism of Malachite Green onto *Luffa aegyptica* peel adsorbent is influenced by the structure and surface properties of the adsorbate and adsorbent. Mashkoor *et al*. [59] conducted an analysis using FTIR and found that the adsorbent surface contains hydroxyl, carbonyl, and amine groups. They proposed that hydrogen bonding may occur between the hydroxyl groups on the adsorbent surface and the nitrogen atoms of Malachite Green. Additionally, electrostatic forces may play a role in the further adsorption of Malachite Green onto the negatively charged adsorbent surface [59]. Hydrogen bonding can occur between the hydrogens of the hydroxyl groups on the adsorbent surface and atoms such as nitrogen and oxygen. Moreover, hydrogen bonding can form between the OH^- groups on the adsorbent surface and the aromatic rings of the cationic dye. In n-π interactions, there are electron donors and acceptors (Figure 5), where the aromatic rings of the dye act as electron acceptors and the oxygens from the adsorbent carbonyl group act as electron donors [60].

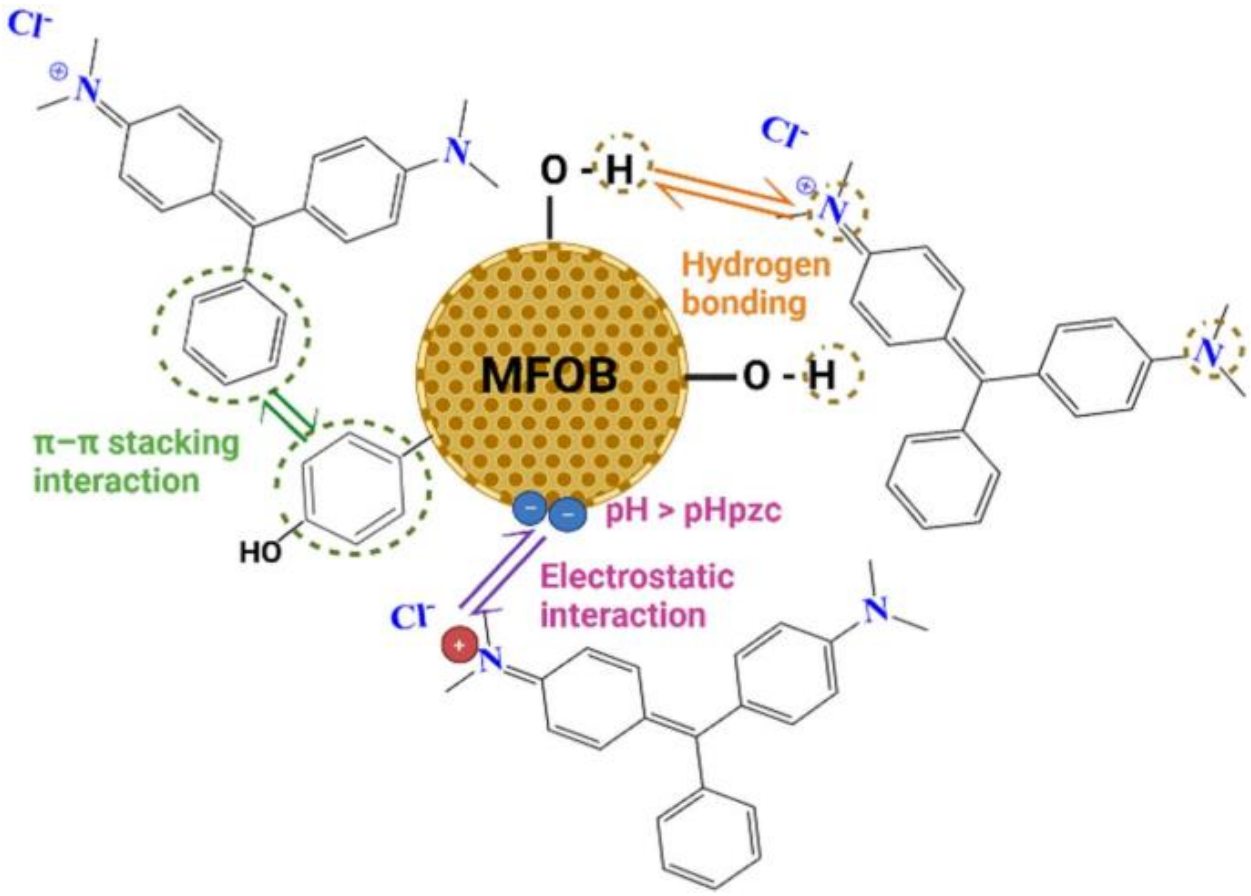

Figure 5: Adsorption mechanism of malachite green

2.9.Factor affecting dye adsorption

Many physicochemical factors influence the amount of adsorption of adsorbate (dye) onto an adsorbent and these include: surface area of adsorbent, initial dye concentration, temperature, P^H and contact time between adsorbate and adsorbent etc.

2.9.1. Effect of pH

The pH factor is very important in the adsorption process especially for dye adsorption. pH of a medium will control the magnitude of electrostatic charges which are imparted by the ionized dye molecules. As a result, the rate of adsorption will vary with the pH of an aqueous solution. At low pH solution, the percentage of dye removal will decrease for cationic dye adsorption, while for anionic dyes the percentage of dye removal will increase. In contrast, at a high solution PH, the percentage of dye removal will increase for cationic dye adsorption and decrease for anionic dye adsorption [61]. For cationic dyes, lower adsorption at acidic pH was due to the

presence of excess H+ ions competing with the pollutant cations for adsorption sites. At higher pH, the acidic functional group on the surface of the adsorbent may get ionized, which enhances the adsorption of positively charged cations through electrostatic attraction. In the case of anionic dyes, the lower pH resulted in higher adsorption as the positively charged surface of the adsorbent could adsorb negatively charged anionic dyes [62].

2.9.2. Effect of adsorbent dosage

The effect of adsorbent dosage on the adsorption process can be carried out by preparing adsorbent-adsorbate solution with different amount of adsorbents added to fixed initial dye concentration and shaken together until equilibrium is attained. The percentage of dye removal increases with increasing adsorbent dosage. Initially the rate of increase in the percent dye removal has been found to be rapid which slowed down as the dose increased. This phenomenon can be explained, based on the fact that at lower adsorbent dose the adsorbate (dye) is more easily accessible and because of this removal per unit weight of adsorbent is higher [63]. However, with rise in adsorbent dose, there is less commensurate increase in adsorption, resulting from many sites remaining unsaturated during the adsorption. But after a certain dosage the increase in removal efficiency is insignificant with respect to increase in dose. This is due to the fact that, at higher adsorbent amount there is a very fast superficial adsorption onto the adsorbent surface that produces a lower solute concentration in the solution than when adsorbent dose is lower. Thus, with increasing adsorbent dose, the amount of dye adsorbed per unit mass of adsorbent is reduced [64].

2.9.3. Effect of Initial concentration

The initial dye concentration is important in adsorption, since a given mass of sorbent material can only adsorb affixed amount of dye. Normally, the dye removal will decrease with increase in initial dye concentration. This is because for a given mass of adsorbent material; the amount of dye that can be adsorbed is fixed. The higher the concentration of the dye, the smaller the volume it can remove. At a low concentration, there will be unoccupied active sites on the adsorbent surface, and when the initial dye concentration increases, the active sites required for adsorption of the dye molecules will be lacking. But the actual amount of dye adsorbed per unit

mass of adsorbent increase with increase in dye concentration. This may be due to the high driving force for mass transfer at a high initial dye concentration [65].

According to the effect of various initial dyes concentration of azo dye on different bio peel was investigated and the investigation showed that percentage of dye adsorption efficiency decreased with increasing of initial dye concentration in the solution. However, the percentage removal of dye is greater at lower initial concentrations and smaller at higher initial concentrations. Thus the adsorption process is highly dependent on the initial concentration of the pollutant [66]. The capacity of the adsorbent material gets exhausted sharply with increase in initial dye concentration. This may be probably as a result of the fact that for a fixed adsorbent dose, the total available adsorption sites remain invariable for all the concentration checked. With increasing concentration the available adsorption sites become fewer and hence the percent removal of dye is dependent upon the initial concentration [67].

2.9.4. Effect of contact time

The effect of contact time on adsorption of dye can be carried out by preparing adsorbent-adsorbate solution with fixed adsorbent dose and initial dye concentration for Different time intervals and shaken until equilibrium. Generally, the rate of removal of dye increases with an increase in contact time to a certain extent. Further increases in contact time do not increase the uptake due to deposition of dyes on the available adsorption site on adsorbent material. At this point, the amount of the dye desorbing from the adsorbent is in a state of dynamic equilibrium with the amount of the dye being adsorbed on to the adsorbent. The time required to attain this state of equilibrium is termed the equilibrium time, And the amount of dye adsorbed at the equilibrium time reflects the maximum adsorption capacity of the adsorbent under those operating conditions [68].

2.9.5. Effect of Temperature

Normally, increasing the temperature leads to a decrease in adsorption due to the adsorbed molecules having greater energies and therefore becoming more likely to release from the surface of the adsorbent. The reason for the fall in the adsorption capacity at elevated temperatures may be at higher temperatures a part of a dye leaves the solid phase and re-enters the liquid phase [69].

2.10. Kinetic Model

In order to determine and interpret the mechanisms of malachite green adsorption processes and the main parameters governing sorption kinetics, several kinetic models are proposed.

2.10.1. Pseudo-first-order kinetics model

A simple kinetic model suggested for the sorption process in solid/ liquid systems is Lagergrens pseudo-first-order expression, which is given as [70]:

$$\frac{dqt}{dt} = K1(qe - qt) \qquad \text{Eq. 1}$$

Where k_1 is the pseudo-first-order rate constant for the adsorption process (min^{-1}), q_e and q_t are the amounts of dye adsorbed per gram of sorbents (mg/g) at equilibrium and at time t (min), respectively. After integration of this kinetic expression for the initial condition of q_t equal to 0, when time (t) approaches 0, its linear form are obtained:

$$\ln(qe - qt) = \ln qe - k1t \qquad \text{Eq. 2}$$

The plot of ln (q_e-q_t) vs t gives a straight line, and pseudo- first-order rate constant k_1 can be calculated from the slope of that line.

2.10.2. Pseudo-second-order kinetics model

The kinetic data also can be analyzed by Ho's pseudo-second-order kinetics model. This model is based on the assumption the sorption follows second order chemisorption, which can be represented in the linear expression as [70]:

$$\frac{t}{qt} = \frac{1}{K2qe^2} + \frac{t}{qe} \qquad \text{Eq. 3}$$

Where K_2 (g/mg min^{-1}) is the rate constant of the pseudo-second order adsorption.

2.11. Adsorption Model

Adsorption isotherm model is essential to understand the adsorption mechanism in a system and predict its behavior. Langmuir and Freundlich isotherms are the most commonly used two-parameter models.

2.11.1. Langmuir model

The Langmuir isotherm was initially developed for gas−solid interaction but is also used for various adsorbents [71]. It is empirical models based on kinetic principles; that is, the surface rates of adsorption and desorption are equal with zero accumulation at equilibrium conditions. Based on the following assumptions, (a) monolayer adsorption, (b) homogeneous sites, (c) constant adsorption energy, and (d) no lateral interaction between the adsorbed molecules, the Langmuir isotherm can be written as;

$$qe = \frac{qoKLCe}{1+KLCe} \qquad \text{Eq. 4}$$

Where q_o is the maximum amount of adsorbed surfactant in mg/ g and K_L is the Langmuir constant in L/mg. The linearized version of Eq. 2 is

$$\frac{Ce}{qe} = \frac{1}{KLqo} + \frac{Ce}{qo} \qquad \text{Eq. 5}$$

A plot between C_e/q_e versus C_e is generate a straight line with a slope of $1/q_o$ and an intercept equals to $1/K_Lq_o$. The monolayer assumption requires identical adsorption sites, and only one molecule can be adsorbed at each site.

2.11.2. Freundlich model

Unlike the Langmuir model, this empirical model can be used for multilayer adsorption on heterogeneous sites. It assumes that the adsorption heat distribution and affinities toward the heterogeneous surface are non-uniform [71]. The mathematical model can be shown as;

$$qe = bC_e^{\frac{1}{n}} \qquad \text{Eq. 6}$$

Where b is the adsorption capacity in L/mg and 1/n is the adsorption intensity or surface heterogeneity. When $0 < 1/n < 1$ adsorption is considered favorable. Unfavorable adsorption occurs when $1/n > 1$ and is irreversible at $1/n = 1$. The linearized form can be written as

$$lnqe = lnb + \frac{1}{n}lnCe \qquad \text{Eq. 7}$$

A plot of ln q_e versus ln C_e produces a straight line with a slope = 1/n and intercept = ln b.

2.12. Characterization Techniques

2.12.1. Fourier Transformation Infrared (FT-IR) Spectroscopy

Infrared spectroscopy is an essential device to characterize the structure of matter at the molecular scale. FT-IR spectroscopy analysis is a method based on the principle of infrared spectroscopy, and it has extended its area of application to the study of biosorbent objects during the last decade [72]. FT-IR Spectroscopy has a large application range, from the analysis of small molecules or a molecular complex to the analysis of complexes (Claudel *et al*., 2020). Infrared spectroscopy probes the molecular vibrations. Functional groups can be associated with characteristic infrared absorption bands, which correspond to the fundamental vibrations of the functional groups [73]. FT-IR spectrometer involves an examination of the twisting, bending, rotation, and vibrational modes of the atoms in a molecule upon interaction with infrared radiation portion of incident radiation are observed at a specific wavelength and function groups of the sample can be identified from the spectrum [74]. FT-IR is very useful to study surface chemistry and identify the possible biomolecules of biosorbents [75]. The possible functional groups that are present in the plant based adsorbent identified in the ranges of 4000-400 cm^{-1} [76].

2.12.2. Scanning electron microscopy (SEM)

The scanning electron microscope is a very useful instrument to get information about topography, morphology, and composition information of adsorbent. It is a type of electron microscope capable of producing high-resolution images of a sample surface. SEM images have a characteristic three-dimensional form and are useful for judging the surface morphology of the sample [77]. This technique provides information regarding the species present at different depths of the sample. SEM may be used to determine the crystallography of (poly) crystalline samples and individual crystallite orientations, as well as crystallographic parameters of the sample. Sample simply deposited onto the top of an adhesive fastened to an aluminum stub/holder. Most often, conductive carbon tape is used to sequester the sample. Computer software was used to collect/analyze the resulting patterns to determine the crystallography of the material. The SEM instrument is based on the principle that the primary electrons released from the source provide energy to the atomic electrons of the specimen, which can then release

as the secondary electrons (SEs) and an image can be formed by collecting these secondary electrons from each point of the specimen.

2.13. Thermodynamic Study

Thermodynamic parameters of adsorption processes are easily evaluated because adsorption is a temperature dependent process [78]. Thermodynamic considerations for adsorption experiments are required in order to establish the spontaneity and feasibility of such processes. Therefore, experimental data obtained from adsorption procedures are employed to determine thermodynamic parameters such as Gibbs free energy change (ΔG_0), change in enthalpy (ΔH_0), change in entropy (ΔS_0), Isosteric heat of adsorption (ΔH_X),adsorption potential (A), hopping number (n), sticking probability (S*) adsorption density (ρ) and activation energy (Ea).

3. MATERIALS AND METHODS

3.1.Experimental Section

Biosorbent preparation and adsorption experiment were conducted at Hawassa University, department of chemistry. SEM and FTIR were done at Adama Science and Technology University and Hawasa University respectively.

3.2.Chemicals and Instruments

3.2.1. Chemical and Reagent

All chemicals were analytical reagent without further purification: malachite green (Samir Tech-Chem, Ltd), phosphoric acid (H_3PO_4 (95% Merck), NaOH (India), 98% H2SO4 (Analytical Reagent, India), 37% HCl (Sigma-Aldrich) and Distilled water were used in this study.

3.2.2. Instrument and Apparatus

The instruments and apparatus selected for this study were: FTIR spectroscopy (PerkinElmer FTIR model spectrum 65) was used for determining functional group of biosorbent. Scanning electron microscopy (SEM Model LEICA S430) was used to determine morphology before and after adsorption of biosorbent, Digital electronic balance (Model JA103P,) with 160 gm loading capacity was used to weigh biosorbent and all other chemicals. Magnetic stirrer hot plate (UK) was used for stirring and maintaining the required temperature. pH meter (MP 220 JENWAY, Japan) used for determination of pH and UV/Vis spectrophotometry (SM-1600 spectrophotometer) was used to determine the concentrations of dye in water sample. Measuring cylinders, dropper, pipettes and micro pipettes (Pyrex, Japan) were used for measuring different volumes of sample solution. Volumetric flasks with stopper (Pyrex, England) for solution preparation, Grinder (China, 2022) were used for grinding sample, aluminum foil, whatman filter paper, spatula, glass tube, wash bottle, hot plate, pestle and mortar were used for grinding and obtained powder sample.

3.3.Sample collection and Sample preparation

3 kg of *Jatropha Curcas* leaf was collected from 01 Kebele, Hawassa city, Sidama Regional state (Figure 6). 01 Kebele was purposively selected depend on the availability of *Jatropha curcas* leaf. The collected *Jatropha curcas* leaf was chopped and cut into small size. Then

washed distilled water several times to removed impurities and dried at room temperature for 15 days. Then dried leaf of the plant was ground into powder and sieved to obtained particle size less than 500 µm [79]. The powder of the plant was used for the preparation of biosorbents.

Figure 6: Sample Collection

3.4.Preparation of biosorbent

A 100 g *Jatropha curcas* leaf powder was soaked in a solution of 0.1 M H_3PO_4, NaOH and H_2SO_4 at 1: 4 (w/v) impregnation ratios for 24 hr. at room temperature. The soaked sample was filtered by whatman filter paper No. 42 and washed with distilled water several times until the pH reached to neutral [24]. The resulting biosorbent was completely dried at 110 °C in an oven for 3 hr. in order to achieve good carbon structure and a large surface area and kept in desiccators for further study.

3.5.Characterization of nanoparticles

3.5.1. Fourier Transform Infrared (FTIR) analysis

FTIR analysis was used to determine functional group of before and after adsorption of biosorbent. The measurement was carried out for 1 mg of powder sample with 100 mg KBr over the range 400−4000 cm^{-1} and pressed into a pellet at a pressure of 1 MPa (mega pascal) [80].

3.5.2. Scanning Electron Microscopy (SEM)

SEM is a powerful magnification technique that utilizes focused beams of electrons to obtain surface morphology of the biosorbent. SEM analysis provides essential information on surface

morphology of before and after adsorption of biosorbent. The fine coarse powder of sample were fixed on a circular metallic sample holder by using double-sided adhesive tape and then the samples was coated with copper using sputter coater for clear visibility of picture, followed by micrographs of surface texture at different magnifications of SEM [81].

3.6. Synthetic wastewater

A 1 g sample of the appropriate MG was dissolved in 1000 mL of distilled water to produce an MG stock solution of 1000 mg/L concentration. The stock solution was then used to prepare MG solutions of concentrations ranging from 10 to 50 mg/L. The initial pH of the stock solution was adjusted by adding to it 0.1 M HCl or NaOH. A 50 ml aliquot of the MG stock solution was used for each of the experiments [1]. All experiments were conducted in triplicate.

3.7.Calibration

The standard solution of 1000 mg/L MG was used to prepare concentrations (10, 20, 30, 40, and 50 mg/L). The absorbance of each dilute concentration of MG was measured by UV/Vis spectrophotometer at wavelength of 617 nm [3]**.**

3.8.Batch Adsorption Experiment

The adsorption experiments were carried out according to [4] with slight modifications. 50 mL (100 mg/L) of synthetic wastewater and 0.5 g adsorbent was taken in 250 mL of conical flask and the desired solutions pH was adjusted with 0.1 M HCl or 0.1 M NaOH for batch experiment. The mixed solutions agitated with magnetic stirrer on digital hot plate at 400 rpm until the required time reached and then the adsorbent was separated from solution by centrifugation at 4000 rpm for 10 min. The concentration of remain supernatants solutions were determined by using UV–Vis spectrophotometer at a maximum wavelength of 617 nm. The removal percentage and adsorption capacity of biosorbent was calculated by:

$$\text{Removal percentage (\%)} = \frac{(Co - Ce)}{Co} \; x \; 100 \qquad \text{Eq. 7}$$

$$q_e = (C_o - C_e)\,\frac{V}{W} \qquad \text{Eq. 8}$$

Where, qe (mg/g) is adsorption capacity, C_o and C_e (mg/l) are the liquid phase concentrations of MG at initial period and equilibrium, respectively. V is the volume (l) of the sample solution and W is the weight (g) of the biosorbent.

3.9.Factor affecting adsorption of MG

Factors affecting adsorption is an important parameters to determine the optimum condition for the adsorption of malachite green from aqueous solution. Factors of adsorption such as pH, adsorbent dosage, initial concentration, temperature and contact time were evaluated [24-25]. The effect of pH for the adsorption of MG in the pH range of 2-12 was studied under the specific condition (30 °C, 120 rpm of agitation speed, adsorbent dose 0.1 g/L, 15 mg/L of initial concentration and 60 min contact time). Adsorbent dosage was varies from 0.05 to 0.3 g, under the specific condition (30 °C, contact time of 120 min, 120 rpm shaking speed and room temperature, 15 mg/L of initial concentration and pH of 6). The effect of initial concentration for the adsorption of malachite green in the range of 10-50 mg/L under specific condition (30 °C, 120 rpm of agitation speed, 0.1 g/L adsorbent dose and pH 6). The effect of contact time for removal of malachite green was studied for the period of 120 minutes at 15 minutes interval under the specific condition (30 °C of Temp, 120 rpm of agitation speed, 15 mg/L of initial concentration, 0.1 g/L of adsorbent dose and pH 6) and Effect of temperature was evaluated in the 25-55°C under specific condition (20 rpm of agitation speed, 15 mg/L of initial concentration, 0.1 g/L adsorbent dose and pH 6) . Then suspension was filtered using watchman filter paper No.42 and analyze by using UV/Vis spectrophotometer.

3.10. Kinetic model

The highest performing adsorbents from the 120 min batch study were assessed for the rate at which they adsorb MG, using a kinetic study. Replicate vials for each material were sampled at times of 0, 15, 30, 45, 60, 75, 90, 105 and 120 minutes [28]. The common kinetic models such as pseudo first order [82] and pseudo second order [83] and the one with the best fit with the experimental data, for MG were used to describe the adsorption mechanism and adsorption rates.

Pseudo-First Order (PFO): $q_t = q_e(1 - e^{-k1t})$ Eq. 9

Pseudo-Second Order (PSO): $q_t = \frac{K_{2q_e^2t}}{1+K_{2q_et}}$ Eq. 10

Where, qt is the amount of 2, 4-D adsorbed at a time "t" (mg· g^{-1}), while k_1 and k_2 are the rate constants for the PFO (min^{-1}) and PSO (g· mg^{-1}· min^{-1}) models, respectively.

3.11. Adsorption model

Once an optimum time was identified from the kinetics experiments, an adsorption test was conducted for the mediation capability of the selected media were assessed across an adsorbent range of 0.05-0.3 g/L, using a MG solution at concentration of 10 ppm for 90 minutes [27]. Common adsorption models such as Langmuir model [84] and Freundlich models [85] were employed to evaluate the fitness quality of each equation with the adsorption data.

$$\text{Langmuir Equation:} \quad q_e = \frac{q_{max} K_{LC_e}}{1+K_{LC_e}} \qquad \text{Eq. 11}$$

$$\text{Freundlich Equation: } K_f(C_e)^{1/n} \qquad \text{Eq. 12}$$

Where, qmax is the Langmuir maximum adsorption capacity (mg· g^{-1}), whereas K_L (L· mg^{-1}), and K_f ($mg^{(1-1/n)}$ .g^{-1} $L^{1/n}$) are coefficients related to Langmuir adsorption, Freundlich affinity respectively. In addition, n is the Freundlich empirical constant.

3.12. Thermodynamic Study

The thermodynamic parameters that help us to understand the nature of the adsorption of MG on [28] adsorbents are the standard change in Gibbs free energy (ΔG°), the standard change in entropy (ΔS^o), and the standard change in enthalpy (ΔH^o). These can be determined using the following equations:

$$\Delta G = -RTlnKc \qquad 13$$

Where R is the gas constant (8.314 J/ mol. K), T is the absolute temperature in Kelvin; And Kc (L/g) is the standard Thermodynamic equilibrium constant defined by qe/Ce. Similarly, the enthalpy change H°) from 298 to 318 K was computed from the following equation:

$$lnkc = \frac{qe}{ce} \qquad 14$$

ΔH° ($kJ.mol^{-1}$) and ΔS° (kJ.mol"^{1}.K"^{1}) were calculated from the slope and intercept of the linear plot of lnkc versus 1/T.

3.13. Method of Validation

3.13.1. Limit of detection (LOD) and Limit of quantification (LOQ)

Limit of detection (LOD) is determined by the analysis of samples with known analyte levels as stated in Eq. (15), where "s" is the standard deviation from samples without analyte, and "b" is the slope of calibration curve equation ([86]. Limit of quantification (LOQ) [86] was determined according to Eq. (16), where "b" is the slope from the calibration curve and "s" is the standard deviation calculated from three blank samples (no analyte added).

$$\mathrm{LOD} = 3.3S/b \quad \text{Eq. 15}$$

$$\mathrm{LOQ} = 10S/b \quad \text{Eq. 16}$$

3.13.2. Recovery test

Accuracy [86] was evaluated by the recovery method analyzing three different concentrations of MG solutions (25 mg L^{-1}). Sample was analyzed by UV–Vis spectrometry in triplicate and the accuracy was determined based on recovery percentage. Recovery percentage was calculated as;

$$\mathrm{Recovery\%} = \frac{\text{amount of spiked} - \text{amount of unspiked}}{\text{amount of added}} \times 100 \quad \text{Eq. 17}$$

4. RESULT AND DISCUSSIONS

4.1.Characterization Biosorbent

4.1.1. Fourier Transform Infrared (FTIR) analysis

FT-IR analysis of biosorbent based of *Jatropha curcas* leaf was presented in Figure 7. The FTIR spectra of before adsorption revealed various functional groups detected on the surface of biosorbent. The broad band at 3478 cm^{-1} corresponded to O–H stretching of hydroxyl group which revealed the presence of phenols. The band at 2322 cm^{-1} is stretching vibrations of carbon to carbon triple bond of alkyne, the band at 1627 cm^{-1} assigned to C=C or C=O indicate the presence of aromatic compound, lignin and aldehyde or ketone compound. The peak at 1322 cm^{-1} corresponding to C-N stretch revealed the presence of aromatic amines compound. The band at 1000-500 cm^{-1} assigned to C–H and C–C bend vibration and halogenated compounds' (C–X) stretching vibration [87]. Similar studies have been reported by Gietu *et al*. [24] and Oyelude *et al*. [55].

The FTIR spectra of after adsorption (Figure 7) revealed that the peaks shifted to 3470, 2328, 1640, 1316, 1082 and 855 cm^{-1} this indicated that the interaction of malachite green with surface functional group of biosorbent [88]. The new peaks observed at the band of 816 cm^{-1} and 770 cm^{-1} correspond to CH out plane deformation and CH out plane deformation (two bands) indicate the affinity of triazines compound and monosubst benzenes compound with malachite green in aqueous solution [89]. The observed changes in IR peaks after MG dye binding indicated that several functional groups on the surface of the biosorbent of *Jatropha curcas* played important roles in interaction with dye, involving of chemisorption process [90].

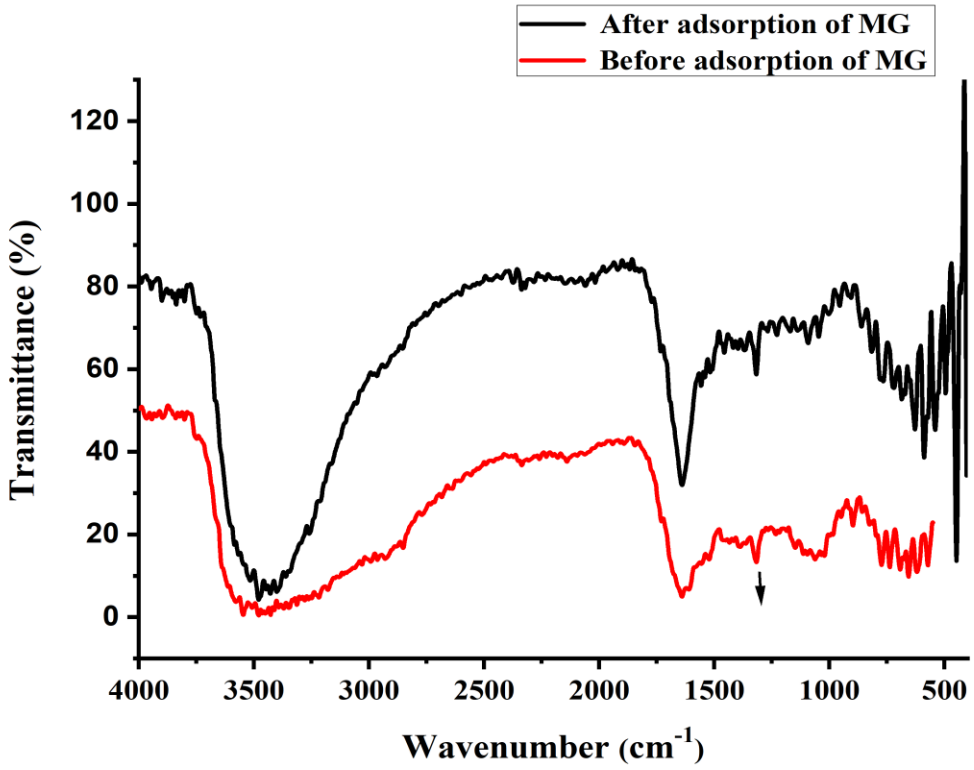

Figure 7: FTIR spectra of before and after adsorption of MG

4.1.2. Scanning Electron Microscopy (SEM) analysis

The SEM was used to assess the surface morphology of before and after adsorption of biosorbent material. As a result, Figure 8A shows that the biosorbent surface is highly irregular, porous, and heterogeneous before adsorption. However, more regular morphology with less cavity and holes were observed after adsorption as shown in Figure 8B. This indicated the successful attachment of the malachite green onto the porous structure of the adsorbent decreasing the porosity as well as cavity. Generally, the SEM analysis revealed that the biosorbent was suitable for removal of malachite green onto their pores. This result is consistent with previous literature report [91-93].

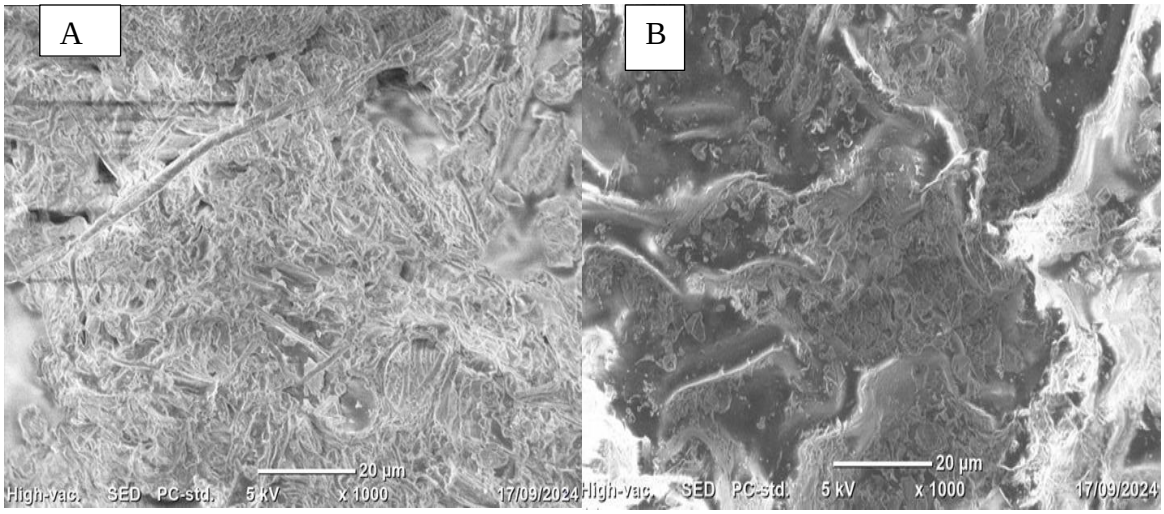

Figure 8: SEM image of before and after adsorption of MG

4.2.Validation method

The calibration curve indicated that correlation coefficients (R^2=0.9972) was close to one with linear equation of y=0.0230x-0.004 (Figure 9). The correlation coefficient of calibration curve presented that proposed method has good linearity for the determination of malachite green from aqueous solution. The results of LOD and LOQ were 0.003 mg/L and 0.01 mg/L respectively (Table 1). The finding of the study revealed that the development method was reliable and effective for analysis of malachite green from aqueous solution [22]. The recovery percentage of MG was 94.9% (Table 1) which found in the acceptable limit of international standard 80-120% [20]. The results indicated that the proposed method used for analysis of malachite green from aqueous solution was accurate.

Table 1: LOD, LOQ and recovery test

	SD	LOD (mg/L)	LOQ (mg/L)	
Phosphate	0.001	0.003	0.01	
Spiked concentration (mg/L)	Amount added (mg/L)		Unspiked concentration (mg/L)	%R
2.187±0.01	2.0		0.289±0.01	94.9

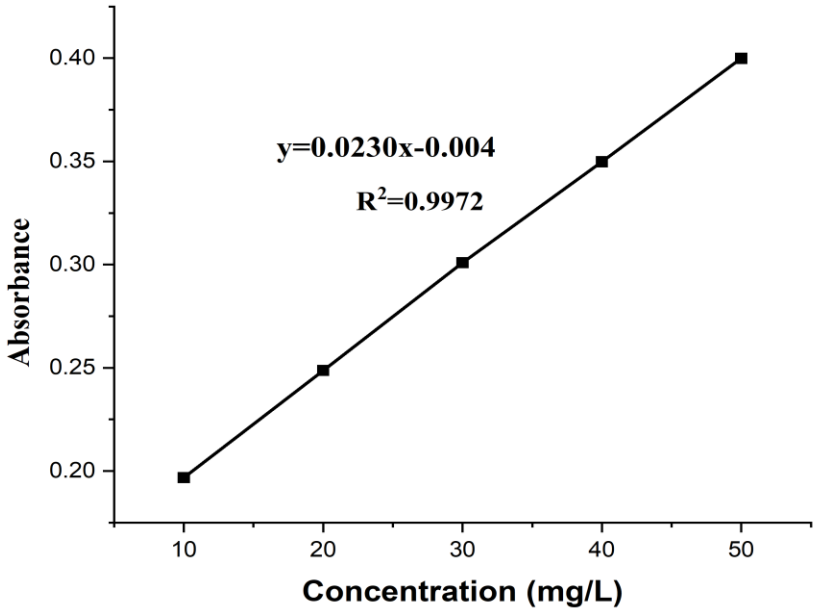

Figure 9: Calibration curve of malachite green

4.3.Optimization parameters

4.3.1. Effect of pH

Effect of pH for the removal of MG were in the range of 2-12 under constant parameters of 30 °C, 120 rpm of agitation speed, adsorbent dose 0.1 g/L, 15 mg/L of initial concentration and 60 min contact time was mentioned in Figure 10. The maximum removal efficiency of malachite green was 95.67 % on the surface of biosorbent was reached at pH 8. Removal efficiency increase with increasing solution pH until equilibrium reached. This is due to increasing pH leads to the formation of negative charge on the surface of adsorbent up on deprotonation reaction. This negative charge enables high removal efficiency as result of electrostatic attraction between the adsorbent and positively charged of adsorbate (MG). Whereas at lower pH, the various functional groups and reactive atom of dyes and adsorbent protonated and both get positive charge [54-55]. Therefore, due to strong repulsive force between dyes and adsorbent decrease the removal percentage. As shown in Figure 10 at acidic region (pH=2) the removal efficient was 66.23% whereas at the basic region (pH=8) was 95.67%. The removal efficiency was increase until the pH reaches to optimum beyond that slightly decrease due to competency of active site of the adsorbent [54]. The optimum pH was 8 for the removal of MG from aqueous solution. The finding of the study similar with the study of Hammud *et al*. (2023) [25] reported

that maximum removal efficiency of malachite green was 88% on the surface of hydrothermal carbonization biochar reached at pH 8.

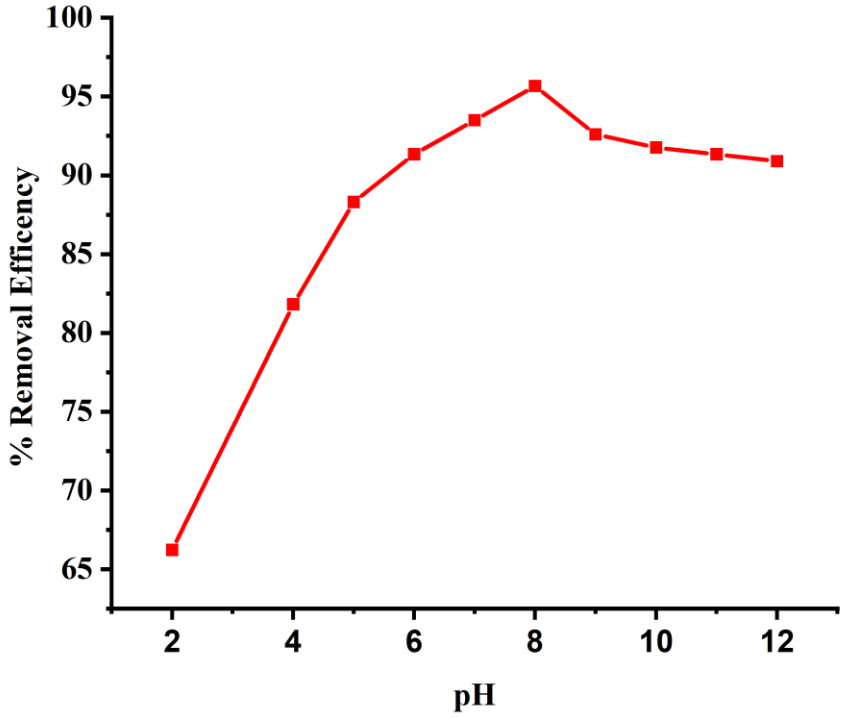

Figure 10: Effect of pH

4.3.2. Effect of Adsorbent Dose

Effect of adsorbent dosage for the removal of MG was studied in the range of 0.05 to 0.3 g/L under constant parameters at 30 °C, 120 rpm of agitation speed, pH 8, initial concentration 15 mg/L and 60 min contact time was represented in Figure 11. The removal efficiency of MG by *Jatropha curcas* biosorbent was increased from 56.27% to 94.80 % as biosorbent doses increased from 0.05 g to 0.2 g/L. The maximum removal efficiency of MG was 94.80% recorded at 0.2 g/L dose. As the adsorbent dosage increases leads to an increase on the surface due to more active sites are available to bind malachite green from aqueous phase [17]. After 0.2 g/L, the amount of MG slightly decreased due to the aggregation and overlapping of particles of adsorbent in the solution, consequently, decrease in the surface for dye uptake occurs. This result is in agreement with data reported by different scholar findings [18-19]. The optimum adsorbent dose for the removal of malachite green from aqueous solution was 0.2 g/L.

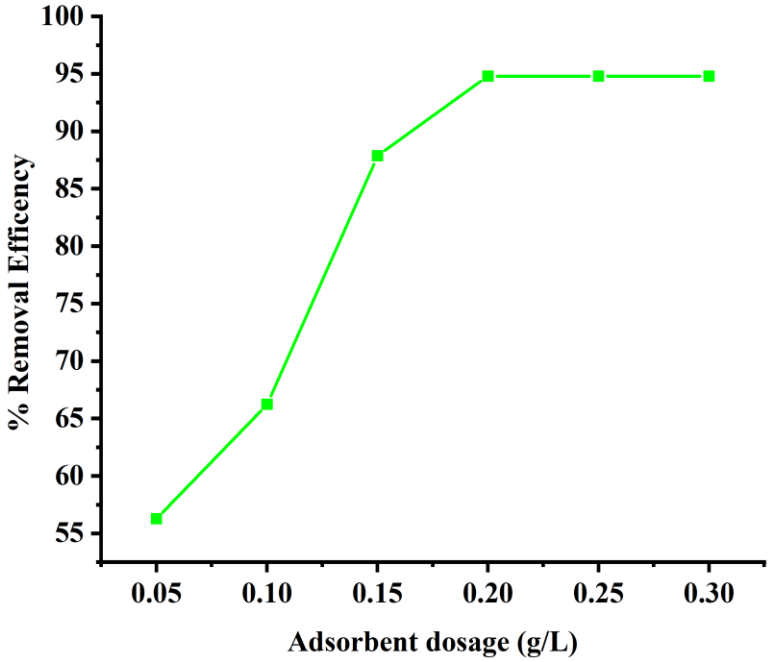

Figure 11: Effect of adsorbent dosage (g/L)

4.3.3. Effect of Initial Dye Concentration

Effect of initial concentration for the removal of MG was studied in the range of 10-50 mg/L under constant parameters condition at 30 °C, 120 rpm of agitation speed, pH 8, 0.2 g/L adsorbent dosage and 60 min contact time was discussed in Figure 12. The removal efficiency of malachite green was decrease from 95.23 % to 74.75 % due to reduction of active sites on the surface of biosorbent [23]. The maximum removal efficiency of MG was 95.23% obtained at 10 mg/L. As shown in Figure 12 removal percentage of MG decrease with increasing initial concentration of malachite green. Since the adsorbent dose is fixed, there is a fixed number of active site for removal of MG was decrease with increasing concentration [25]. At low initial concentrations of MG dye relatively high removal efficiency of MG was obtained. As a result of the high ratio of adsorbent surface binding sites to the dye concentration, meaning that a fewer number of malachite green was competing for the available binding sites on the adsorbent [54]. The optimum initial concentration for removal of malachite green from aqueous solution was 10 mg/L.

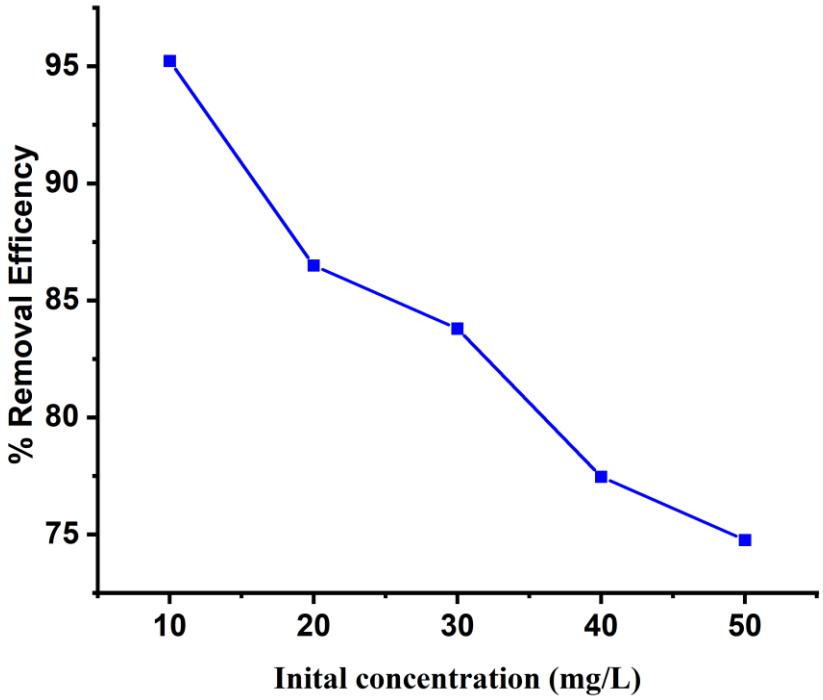

Figure 12: Effect of initial concentration

4.3.4. Effect of Contact Time

Contact time is an important factor in MG adsorption. A comprehensive investigation was performed to explore the effect of contact time adsorption over time periods ranging from 15 to 120 minutes under specific condition of 120 rpm of agitation speed, 0.2 g/L adsorbent dose, 10 mg/L of initial concentration and pH 8. Initially the removal rate of MG by biosorbent was rapid as described in the Figure 13 with distinct pattern. By increasing the duration of contact between MG and biosorbent, the removal efficiency significantly enhance because of the increased interaction between MG and adsorption active sites [1]. Typically, at the start of the adsorption process, the Removal efficiency starts off fast and then builds up progressively. This happens as a result of the accessibility of the initial free active sites available for adsorption, which is progressively taken up by adsorption MG over time [93]. The maximum removal percentage of MG was 95.67% at 90 minutes. The optimal contact time for the removal of MG was 90 min.

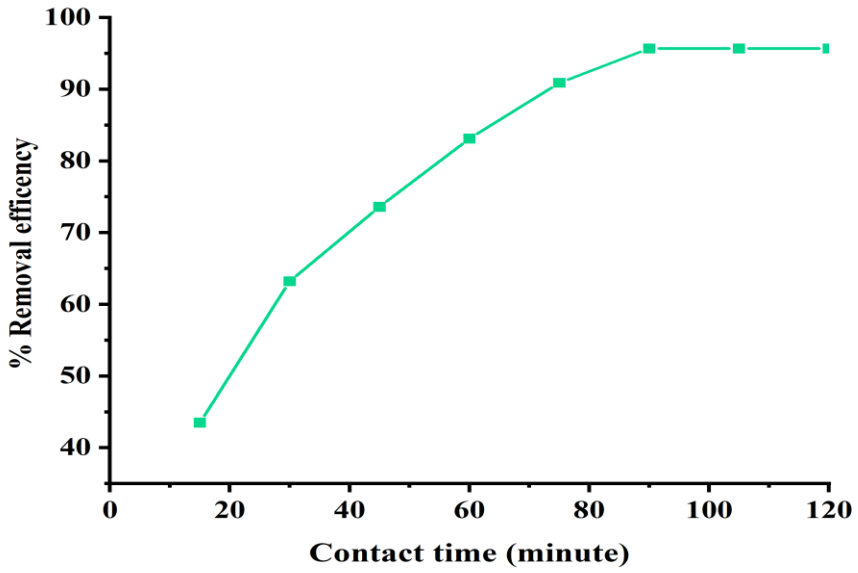

Figure 13: Effect of contact time

4.3.5. Effect of temperature

Figure 14 explained the effect of temperature ranging from 25 to 55°C for the removal of MG at constant parameters of 120 rpm of agitation speed, 0.2 g/L adsorbent dose, pH 8, 10 mg/L initial concentration and 90 minutes. The result of the study revealed that the increase in temperature leads to the increase in removal percentage of malachite green from aqueous solution. The adsorption is an endothermic process; as the temperature increases, the adsorption equilibrium shifts directly or the concentration of the adsorbent in the solution is increased, leading to an increase in the adsorption efficiency and capacity. The maximum removal percentage of MG was 95.5% reached at 45 °C. This may be due to the fact that at higher temperatures the solute molecules show an inclination to escape from the solid phase and reenter the liquid phase due to increased mobility [94].

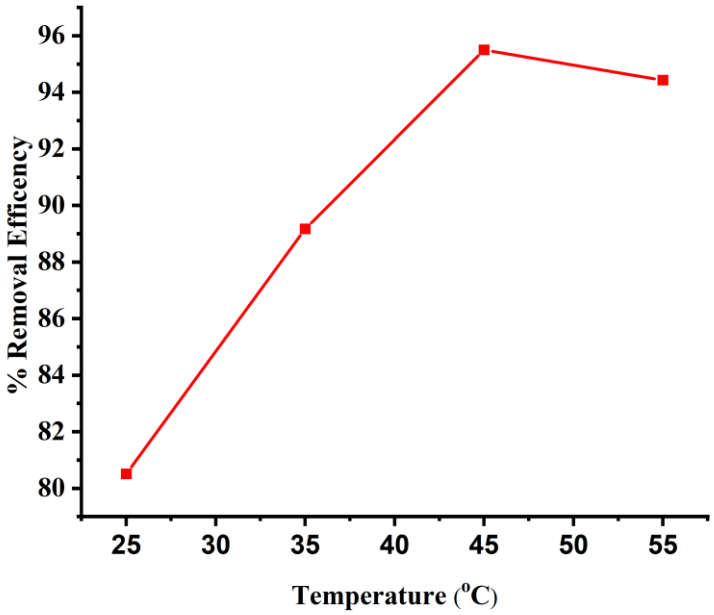

Figure 14: Effect of temperature

4.4.Removal percentage and Adsorption capacity

Removal efficiency and adsorption capacity of MG by *Jatropha curcas* leaf biosorbent was shown in Table 2. The removal efficiency of MG was 99.6% and adsorption capacity was 49.8 mg g^{-1} respectively. The results revealed that biosorbent has higher removal efficiency and adsorption capacity of MG from aqueous solution due to its better surface functional group, surface morphology and availability of binding sites on the surface of biosorbent [20].

Table 2: Removal percentage and adsorption capacity of MG

C_i	C_e	RE%	Q_e (mg/g)
100	**0.4**	**99.6**	**49.8**

4.5.Kinetic model

Kinetics model investigates the rate of adsorption as an important time-dependent parameter for the modeling and design of adsorption processes of MG as shown in Figure 15. Table 3 presented kinetic parameters for the adsorption of MG using pseudo first order (PFO) and pseudo second order (PSO) models. Pseudo second order model best fits for the removal of malachite green from aqueous solution due to higher correlation coefficient and lower sum square error (R^2: 0.99999, SSE: 0.000051). It can be seen that the correlation coefficient (R^2) for PSO is

closer to unity than PFO (R^2: 0.96, SSE: 1.15). Then Pseudo first order model less fits for the removal of Malachite Green from aqueous solution. The q_{cal} of pseudo second order were 43.63 mg/g close to experimental adsorption capacity (49.8 mg/g). *Jatropha curcas* leaf biosorbent has faster removal rate of malachite green from aqueous solution due to its higher rate constant (0.11 g mg^{-1} min^{-1}). The suitability of the PSO model is a suggestion that the adsorption of MG^{-} molecules onto *Jatropha curcas* leaf biosorbent was controlled by electron transfer between the adsorbent surface and the adsorbate which is known as chemical adsorption. This implies that the MG molecules were bonded to the active sites on the surface of the adsorbent by a chemical bond reported previously in the literature [9-13].

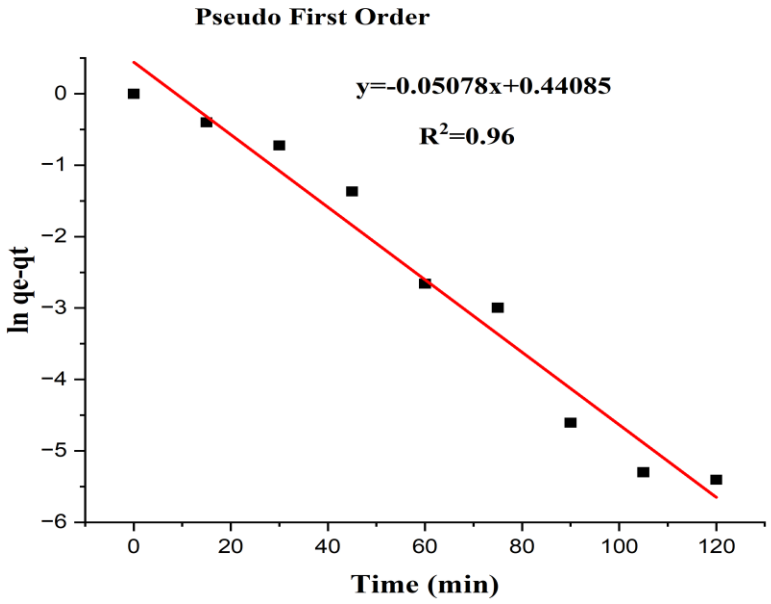

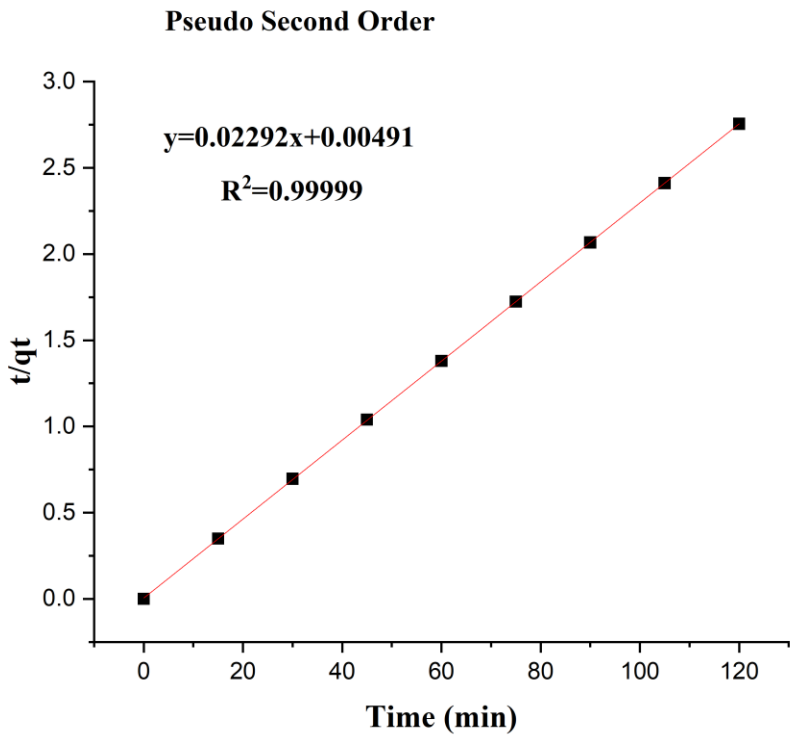

Figure 15: Kinetic model

Table 3: Parameters of Kinetic model

Pseudo first order			
qe(mg/g)	**K_1 (min^{-1})**	**R^2**	**SSE**
1.55	**-0.0004**	**0.96**	**1.15**
Pseudo second order			
qe (mg/g)	**K_2 (g mg^{-1} min^{-1})**	**R^2**	**SSE**
43.63	**0.11**	**0.99999**	**0.000051**

4.6.Adsorption models

The adsorption model was used to determine the adsorption of Malachite Green on surface of biosorbent was discussed in Figure 16. In this study the most common adsorption models (Langmuir and Freundlich) were analyzed. The adsorption model parameter was given in Table 4. In this study Freundlich model more fits for the adsorption of MG from aqueous solution due to its higher correlation coefficients and lower mean standard error (MSE) (R^2:0.99993, MSE:0.000055) than Langmuir model (R^2:0.97, MSE: 0.00025). Freundlich model with

maximum adsorption coefficient K_f=1.13 mg^{1-n} L^n g^{-1} and intensity of adsorption (1/n) in Table 4 greater than zero and lower than 1, ($0 < 1/n < 1$) (1/n: 0.68) revealed that the adsorption process is favorable [19]. It showed that multilayer adsorption process occurred on the surface of biosorbent which responsible for the adsorption of malachite green from aqueous solution [91]. The finding of the study in good agreement with previous literature report [5, 23, 25, 92] reported that Freundlich model was best fit model than Langmuir model for the removal of MG from aqueous solution on the surface biosorbent.

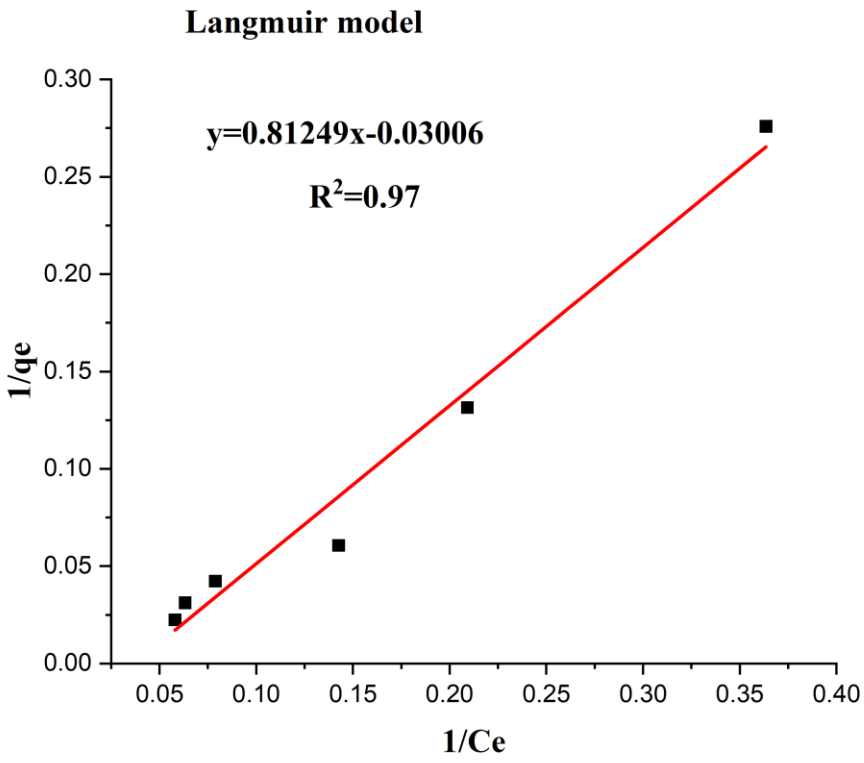

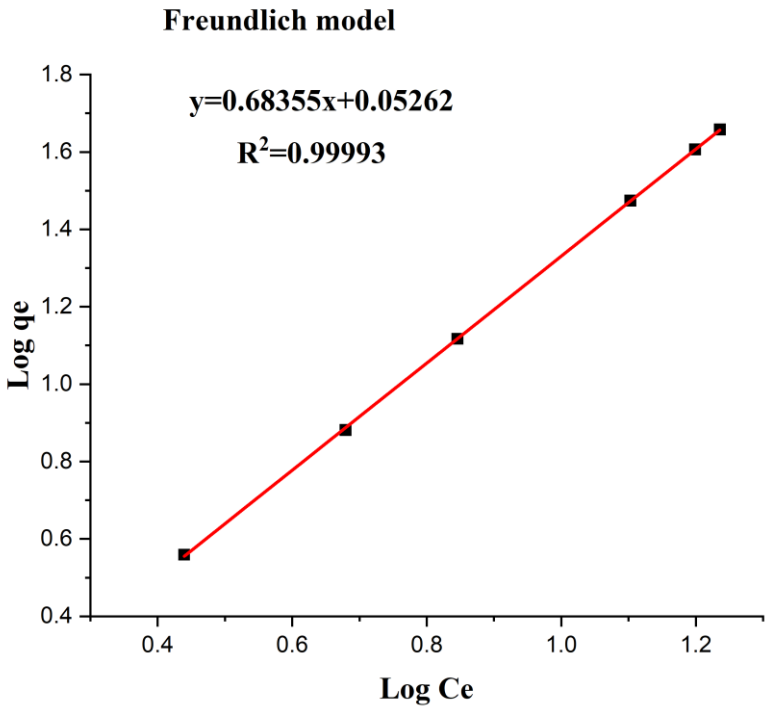

Figure 16: Adsorption model

Table 4: Parameters of adsorption model

Langmuir model				
q_{max} (mg/g)	**K_L**	**R_L**	**R^2**	**MSE**
-33.27	**-0.04**	**-1.18**	**0.97**	**0.00025**
Freundlich model				
K_f	**1/n**	**R^2**	**MSE**	
1.13	**0.68**	**0.99993**	**0.000055**	

4.7.Thermodynamic study

The positive value of enthalpy change confirms the endothermic nature of the adsorption process (Table 5 and Figure 17). The enthalpy value for adsorption process used to distinguish between chemical and physical adsorption. For chemical adsorption, values of enthalpy change range from 83 to 830 kJ/ mol [88], while for physical adsorption they range from 8 to 25 kJ/ mol [86]. The low values of ΔH give clear evidence that the interaction between MG and adsorbent was less effective. Then MG adsorption by biosorbent is a physical adsorption process. The positive value of entropy, ΔS° represents an increase in the degree of freedom of the adsorbed species.

The positive value of ΔS° also reflects that some changes occur in the internal structure of biosorbent during the adsorption process. The magnitude of Gibbs free energy change, ΔG° obtained is negative demonstrating that the adsorption is rapid and spontaneous. The negative value of ΔG° ensures the feasibility of the process [90].

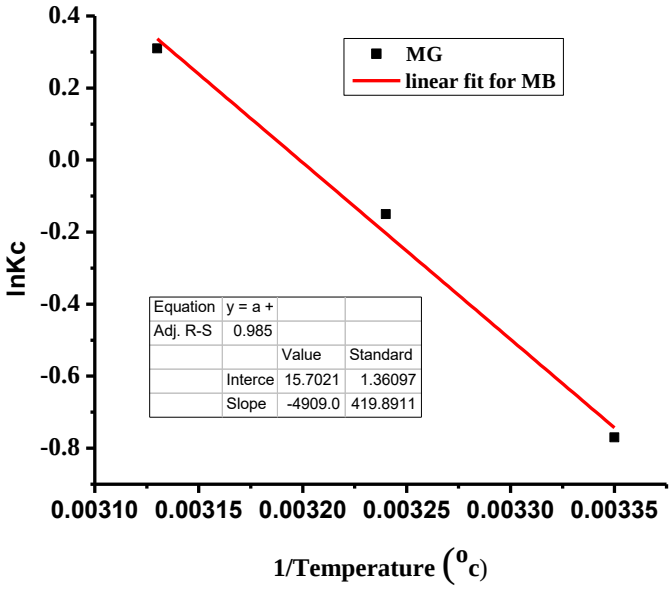

Figure 17: van Hoff plot

Table 5: Thermodynamic parameters

T (K)	Lnkc	ΔG(KJ/mol)	ΔH (KJ/mol)	ΔS(J/mol.k)
298	-0.77	- 1907.7	40813.42	130.52
308	-0.15	- 384.1		
318	0.048	-126.9		

5. CONCLUSION AND RECOMMENDATIONS

5.1.Conclusion

In this study biosorbent was successfully prepared from *Jatropha curcas leaf* via chemical activation method. Biosorbent were characterized using FTIR and SEM analytical techniques. The FTIR analysis showed the presence of phenols, aromatic compound, lignin, ketone and aldehyde and also the after adsorption spectra showed the interaction between malachite green and biosorbent. SEM analysis confirmed the irregular, porous, heterogeneous and after adsorption shows that great interaction of malachite green with biosorbent. The removal percentage and adsorption capacities of malachite green from aqueous solution was 99.6% and 49.8 mg/g was obtained at optimal condition of pH 8, 10 mg/L of initial concentration, 0.2 g/L of adsorbent dosage, 90 minutes of contact time and 45 ℃. Freundlich model was best fit for removal of malachite green from aqueous solution than Langmuir due to its higher correlation coefficients and lower mean standard error (MSE) (R^2: 0.99993, MSE:0.000055). Pseudo second order was well fitted for the adsorption of malachite green from aqueous solution than pseudo first order due to its higher coefficients and lower sum square error (SSE) (R^2:0.99999, SSE: 0.000051). Thermodynamic process revealed that adsorption of malachite green from aqueous solution was spontaneous process and endothermic reaction at temperatures of 298, 308 and 318 K. Therefore the findings of the study revealed that novel biosorbent was cost-effective and efficient adsorbent for removal of malachite green from aqueous solution.

5.2.Recommendation

Depend on the finding of the study to recommended the following issues; Thus, this work consider biosorbent as being good alternative less expensive materials for purification of water from malachite green. In future *Jatropha curcas* leaf biosorbent was effective for the removal of malachite green, then researcher should check its efficacy on the real water sample. Further research must be undertaken on biosorbent for various pollutants removal, as evaluated in this study, to transfer from the laboratory scale to the mass production. Future research should focus on the usability of *Jatropha curcas* leaf biosorbent in large-scale wastewater treatment. Also to recommended that toxic products on the environmental compartments can further exacerbate water pollution hence the need to prevent their occurrence through biosorbent.

6. REFERENCES

1. Moustafa, M. T. 2023. Preparation and characterization of low-cost adsorbents for the efficient removal of malachite green using response surface modeling and reusability studies. *Scientific Reports* 13:4493.
2. Puchongkawarin, C., S. Mattaraj and C. Umpuch. 2021. Experimental and modeling studies of methylene blue adsorption onto nabentonite clay. *Eng. Appl. Sci. Res.* 48(3): 268-279.
3. Tarekegn, M. M and M. Balakrishnan. 2021. Zerovalent iron, nanoclay and iron impregnated. 30109-30131. https://doi.org/10.1039/d1ra03918k
4. Arunprasath, T., S. Sudalai, R. Meenatchi, K. Jeyavishnu and A. Arumugam. 2019. Biocatalysis and Agricultural Biotechnology Biodegradation of triphenylmethane dye malachite green by a newly isolated fungus strain. *Biocatal. Agric. Biotechnol.* 17: 672-679.
5. Akpomie, K. G and J. Conradie. 2020. Efficient synthesis of magnetic nanoparticle-*Musa acuminata* peel composite for the adsorption of anionic dye. *Arab. J. Chem.* 13(9): 7115-7131. https://doi.org/10.1016/j.arabjc.2020.07.017
6. Vergis, B. R., et al. 2018. Removal of malachite green from aqueous solution by magnetic CuFe2O4 nano-adsorbent synthesized by one pot solution combustion method. *J. Nanostruct. Chem.* 8(1): 1-12. https://doi.org/10.1007/s40097-017-0249-y
7. Kabeer, F. A., N. John and M. H. Abdulla. 2019. Biodegradation of malachite green by a newly isolated *Bacillus vietnamensis* sp. MSB17 from continental slope of the Eastern Arabian Sea: Enzyme analysis, degradation pathway and toxicity studies. *Bioremediat. J.* 23(4): 334–342. https://doi.org/10.1080/10889868.2019.1671790
8. Sutar, S. S., et al. 2019. Biocatalysis and Agricultural Biotechnology Biodegradation and detoxification of malachite green by a newly isolated bioluminescent bacterium *Photobacterium leiognathi* strain MS under RSM optimized culture conditions. *Biocatal. Agric. Biotechnol.* 20:101183.
9. Omar, H., A. El-gendy and K. Al-ahmary. 2018. Bioremoval of toxic dye by using different marine macroalgae Bioremoval of toxic dye by using different marine macroalgae. *Turk. J. Bot.* https://doi.org/10.3906/bot-1703-4

10. Ali, I. 2018. Phytogenic magnetic nanoparticles functionalized. *RSC Adv.* https://doi.org/10.1039/c8ra00245b
11. Chaturvedi, V and P. Verma. 2015. Biodegradation of malachite green by a novel copper—Tolerant *Ochrobactrum pseudogrignonense* strain GGUPV1 isolated from copper mine waste water. *Bioresour. Bioprocess.* https://doi.org/10.1186/s40643-015-0070-8
12. Yong, L., et al. 2015. Photodegradation of malachite green under simulated and natural irradiation: Kinetics, products, and pathways. *J. Hazard. Mater.* 285: 127-136. https://doi.org/10.1016/j.jhazmat.2014.11.041
13. Du, J., L. Zhang, H. Gao and Y. Liao. 2017. Removal of methylene blue from aqueous solutions using Poly(AA-co-DVB). *J. Dispers. Sci. Technol.* 38(10): 1489-1494. https://doi.org/10.1080/01932691.2016.1255955
14. Argumedo-delira, R and J. G. Mario. 2021. Applied sciences trichoderma biomass as an alternative for removal of Congo Red and Malachite green industrial dyes. *Appl. Sci.* 11: 448.
15. Roy, D. C., et al. 2020. Isolation and characterization of two bacterial strains from textile effluents having Malachite Green dye degradation ability. *bioRxiv* https://doi.org/10.1101/2020.03.29.014274
16. Shamsizadeh, A., M. Ghaedi, A. Ansari, S. Azizian and M. K. Purkait. 2014. Tin oxide nanoparticle loaded on activated carbon as new adsorbent for efficient removal of malachite green-oxalate: Non-linear kinetics and isotherm study. *J. Mol. Liq.* 195: 212-218.
17. Saleh Bashanaini, M. 2019. Removal of Malachite green dye from aqueous solution by adsorption using modified and unmodified local agriculture waste. *Sci. J. Anal. Chem.* **7**(2):42. https://doi.org/10.11648/j.sjac.20190702.12
18. Zubir, M., et al. 2020. Preparation and characterization of *Jatropha curcas* leaves as a biosorbent for Pb(II) and Cd(II) removal in liquid waste. *Journal of Physics: Conf. Series* 1460:012080.
19. Khatab, E. T and S. D. Salman. 2023. Removal of malachite green from aqueous solution using *Ficus benjamina* activated carbon-metal oxide synthesized by pyrocarbonic acid microwave. *Desalination and Water Treatment* 302:195-209.

20. Pudza, M. Y and Z. Z. Abidin. 2020. A sustainable and eco-friendly technique for dye adsorption from aqueous media using waste from Jatropha curcas (isotherm and kinetic model). *Desalination and Water Treatment* 182:365-374.
21. Nacke, H., A. C. Goncalves, G. F. Coelho, et al. 2017. Removal of Cd (II) from water using the waste of jatropha fruit (Jatropha curcas L.). *Appl Water Sci* 7:3207-3222.
22. Saad, T. M. 2024. Grass Waste: A Highly Biosorbent for the Removal of Malachite Green Dye From Aqueous Solution. *Asian Journal of Green Chemistry* 8:349-359.
23. Ashish S. S., et al. 2017. Removal of malachite green dye from aqueous solution with adsorption technique using *Limonia acidissima* (wood apple) shell as low cost adsorbent. *Arabian Journal of Chemistry* 10: S3229-S3238.
24. Gietu, Y. A., N. A. Adugna, T. H. Adere and M. G. Desiew. 2020. Adsorptive removal of malachite green dye from aqueous solution onto activated carbon of *Catha edulis* stem as a low cost bio-adsorbent. *Environ Syst Res.* 9:29.
25. Hammud, H.H.; Hammoud, M.H.; Hussein, A.A.; Fawaz, Y.B.; Abdul Hamid, M.H.S.; Sheikh, N.S. 2023. Removal of Malachite Green Using Hydrochar from PALM Leaves. *Sustainability* 15: 8939.
26. Dawood, S and T. K. Sen. 2014. Review on Dye Removal from Its Aqueous Solution into Alternative Cost effective and Non-Conventional Adsorbents. *Journal of Chemical and Process Engineering* 1(104): 1-11.
27. Dwivedi, C.P., J. N. Sahu, C. R. Mohanty and B. R. Mohan B.R. 2008. Column performance of granular activated carbon packed bed for Pb (II) removal. *Journal of hazardous materials* 156(1-3): 596-607.
28. Encinar, J.M.; F. J. Beltran and A. Ramiro. 1998. Pyrolysis/gasification of agricultural residues by carbon dioxide in the presence of different additives: influence of variables. *Fuel Processing Technology* 55(3): 219 -231.
29. Eren, E. 2009. Investigation of a basic dye removal from aqueous solution onto chemically modified Unye bentonite**.**
30. Fasust, S., A. Dand and M. Osman. 2004. Adsorption Processes for Water treatment, Butter worth's, Boston, Massa cusetts. *Chemistry of water* 509:1987-1920.
31. Garba, Z. N., Z. U. Zango, A. Babando and A. Galadima. 2015. Competitive adsorption of dyes onto granular activated carbon. *J Chem Pharm Res*. 7:710-717.

32. Gebeyehu, B. T., D. M. Kabtamu and T. A. Tasew. 2024. Efficient removal of methylene blue dye from aqueous solution using a new biosorbent derived from *Enset eventricosum* (Enset). *Bulletin of the Chemical Society of Ethiopia* 38(1): 69-84.
33. Guo, X., Q. Du, W. Zhang, X. Xin, L. Yan, H. Yu. Removal of basic dyes (malachite green) from aqueous medium by adsorption onto amino functionalized graphenes in batch mode. *Desalination and Water Treatment* 53: 818-825.
34. Abd EI-Latif, M. M., A. M. Ibrahim and M. F. EI-Kady. 2010. Adsorption equilibrium, kinetics and thermodynamics of methylene blue from aqueous solutions using biopolymer oak sawdust composit**e**. *Journal of American Science* 6: 267-283.
35. Raval, N. P., P. U. Shah and N. K. Shah. 2016. Nanoparticles loaded biopolymer as effective adsorbent for adsorptive removal of malachite green from aqueous solution. *Water Conserv Sci Eng*. 1:69-81.
36. Hameed, B.H. 2009. Evaluation of papaya seeds as a novel non-conventional low-cost adsorbent for removal of methylene blue. *Journal of Hazardous materials* 162(2-3): 939-946.
37. Hasan, M. 2008. Adsorption of reactive azo dyes on chitosan/oil-palm ash. M. Sc. thesis, Malaysia University of Science.
38. Liu, J., R. Li and B. Yang. 2020. Carbon Dots: A New Type of Carbon-Based Nanomaterial with Wide Applications. *ACS Cent. Sci*. 6(12): 2179-2195.
39. Kim, S., H. Park, S. Pandey, D. Jeong, C. -T. Lee, J, Y. Do, S. –M. Park and M. Kang, 2022. Effective Antibacterial/Photocatalytic Activity of ZnO Nanomaterials Synthesized under Low Temperature and Alkaline Conditions. *Nanomaterials* 12: 4417.
40. China, C, R., M. M. Maguta, S. S. Nyandoro, A. Hilonga, S. V. Kanth and K. N. Njau. 2020. Alternative tanning technologies and their suitability in curbing environmental pollution from the leather industry. *Chemosphere* 254: 126804.
41. Wang, S., Y. Tang, Z. Du and M. Song. Export trade, embodied carbon emissions, and environmental pollution: An empirical analysis of China's high- and new-technology industries. *J. Environ. Manage*. 276: 111371.
42. Gupta, N. K., Y. Ghaffari, S. Kim, J. Bae, K. S. Kim and M. Saifuddin. Photocatalytic Degradation of Organic Pollutants over MFe2O4 (M = Co, Ni, Cu, Zn) Nanoparticles at Neutral pH. *Sci. Rep*. 10(1): 1-11.

43. Ibrahim, M. B. P. N., S. Datel, M. Roger. 1996. Microbial decolorization of textile dye containing effluents: *a review. Bio resource Technology* 53(3): 217-227.
44. Imam, S. S., R. Adnan, N. H. M. Kaus. 2020. Immobilization of BiOBr into cellulose acetate matrix as hybrid film photocatalyst for facile and multicycle degradation of ciprofloxacin. *Journal of Alloys and Compounds* 155990.
45. Kara, A and E. Demirbel, E. 2021. Kinetic, isotherm and thermodynamic analysis on adsorption of Cr (VI) ions from aqueous solutions by synthesis and characterization of magnetic poly (divinylbenzene-vinylimidazole) micro beads. *Water, Air, and Soil Pollution* 223(5): 2387-2398.
46. Krizanec, B and A. M. L. Marechal. 2006. Dioxins and dioxin-like persistent organic pollutants in textiles and chemicals in the textile sector. *Croatica Chemica Acta*. 79: 177-186.
47. Kushwaha, A. K., N. Gupta and M. C. Chattopadhyaya. 2014. Removal of cationic methylene blue and malachite green dyes from aqueous solution by waste materials of *Daucuscarota. J Saudi Chem Soc*. 18: 200-7
48. Labanda, J., J. Sabate and J. Llorens. Modeling of the dynamic adsorption of an anionic dye through ion- exchange membrane adsorbent**.** *Journal of Macromolecular secience* 340: 234-240.
49. Lee, E. J., W. Yang and H. J. Shin. 2011. Removal of malachite green by adsorption and precipitation using amino propyl functionalized magnesium phyllosilicate. *Journal of Hazards Materials* 792: 62-70.
50. Mondal, N.K., S. Kar. 2018. Potentiality of banana peel for removal of Congo red dyes from aqueous solution: isotherm, kinetics and thermodynamics studies. Applied *Water Science* 8**:** 157.
51. Mukherjee, S. K. S., A. K. Misra and P. C. Acharya. 2006. Removal of Aqueous Nickel (II) Using Laterite as a Low-Cost Adsorbent. *Environmental water Resource* 78: 2268-2275.
52. Murat, M., M. A. Ahmad, M. A and M. Idris. 2018. Optimization of preparation conditions for rice husk based activated carbons for the removal of methylene blue dye. *International journal of petro-chemistry and research* 186-188.

53. Oguz, E. 2005. Adsorption characteristics and the kinetics of the Cr (VI) on the *Thujaoriantalis*. Colloids and Surfaces: *Physicochemical and Engineering Aspects* 252(2-3): 121-136.
54. Abewaa, M., A. Mengistu and T. Takele et al. 2023. Adsorptive removal of malachite green dye from aqueous solution using *Rumex abyssinicus* derived activated carbon. *Sci Rep*. 13: 14701.
55. Oyelude, E.O., J. A. M. Awudza and S. K. Twumasi. 2018. Removal of malachite green from aqueous solution using pulverized teak leaf litter: equilibrium, kinetic and thermodynamic studies. *Chemistry Central Journal* 12: 81.
56. Moumni, B., I. Zouitane, M. Achik, A. Oulmekki, H. Zaitan and N. El Ghachtouli and H. Benmoussa, H. (2024). Effect of lightweight composite brick's waste on the removal of malachite green from aqueous solution and phytotoxicity assessment. *International Journal of Environmental Analytical Chemistry* 1-23.
57. Nethaji, S., Sivasanny, A., Mandal, A. B. (2013). Adsorption isotherms, kinetics and mechanism for the adsorption of cationic and anionic dyes onto carbonaceous particles prepared from Juglans regia shell biomass. International Journal of Environmental Science and Technology, 10(2), 231–242.
58. Tran, H. N., You, S. J., Nguyen, T. V., Chao, H. P. (2017). Insight into the adsorption mechanism of cationic dye onto biosorbents derived from agricultural wastes. Chemical Engineering Communications, 204(9), 1020–1036.
59. Mashkoor, F., Nasar, A. (2019). Preparation, characterization and adsorption studies of the chemically modified Luffa aegyptica peel as a potential adsorbent for the removal of malachite green from aqueous solution. Journal of Molecular Liquids, 274, 315–327.
60. Tran, H. N., You, S. J., Chao, H. P. (2017). Fast and efficient adsorption of methylene green 5 on activated carbon prepared from new chemical activation method. Journal of Environmental Management, 188, 322–336.
61. Salleh. M. 2011. Cationic and anionic dye adsorption by agricultural solid wastes a comprehensive review.
62. Salunkhe, B and T. P. Schuman. 2021. Super-Adsorbent Hydrogels for Removal of Methylene Blue from Aqueous Solution: Dye Adsorption Isotherms, Kinetics, and Thermodynamic Properties. *Macromol.* 1(4): 256-275.

63. Salleh, M.A.M., D. K. Mahmoud and W. A. Karim. 2003. Cationic and anionic dye adsorption by agricultural solid wastes: *A comprehensive review. Desalination* 280:1-13.
64. Almasi, A., F. Navazeshkha and S. A. Mousavi. 2017. Biosorption of lead from aqueous solution onto *Nasturtium officinale* Performance and modeling Biosorption of lead from aqueous solution onto *Nasturtium officinale*. Performance and modeling. *Desalination and Water Treatment* 65:443-450.
65. Roy, A., S. Chakraborty, S. P. Kundu, B. Adhikari and S. B. Majumder. 2012. Adsorption of anionic-azo dye from aqueous solution by lignocellulose- biomass jute fiber: Equilibrium, kinetics, and thermodynamics study. *Industrial and Engineering Chemistry Research* 51(37): 12095-12106.
66. Saeed, M. S and M. Iqbal. 2010. Application potential of grapefruit peels as dye sorbent: Kinetics, equilibrium and mechanism of crystal violet adsorption. *Journal of Hazards Materilas* 779: 564-572.
67. Sahu, A. W. O. 2014. Removal of Reactive Dye from Aqueous Solution Using Physico-Chemically Treated Rice Husk. *Science* 2: 77-84.
68. Sivakumar, S., P. Senthilkumar and V. Subburam. 2001. Carbon from cassava peel, an agricultural waste, as an adsorbent in the removal of dyes and metal ions from aqueous solution. *Bioresource technology* 80(3): 233-257.
69. Soni, M., A. K. Sharma, J. K. Srivastava and J. S. Yadav. 2012. Adsorptive removal of Methylene blue dye from an aqueous solution using water hyacinth root powder as a low cost adsorbent. *Int. J .Chem. Sci. Appl*. 3(3):338-345.
70. Xu, Q., W. Li, L. Ma, D. Cao, G. Owens and Z. Chen. 2019. Simultaneous removal of ammonia and phosphate using green synthesized iron oxide nanoparticles dispersed onto zeolite. *Science of the Total Environment*.
71. Akram, M., X. Xu, B. Gao, S. Wang, R. Khan, Q. Yue, P. Duan, H. Dan and J. Pan. 2021. Highly efficient removal of phosphate from aqueous media by pomegranate peel co-doping with ferric chloride and lanthanum hydroxide nanoparticles. *Journal of Cleaner Production* 292: 125311.
72. Baudot, C., C. Ming and J. Chien. 2010. Infrared Physics and Technology FT-IR Spectroscopy as a Tool for Nano-Material Characterization. *Infrared Phys. Technol*. 53: 434-438.

73. Voloshin, Y., I. Belaya and R. Kramer. 2016. The Encapsulation Phenomenon.
74. Xavier, S., V. Lakshmi, R. M. Jenila. 2019. EPRA International Journal of Research and Development (IJRD) synthesis of Nio nanoparticles using *thespesia populnea* leaves by green 7838.
75. Nagajyothi, P. C., S. V. P. Vattikuti, K. C. Devarayapalli, K. Yoo, et al. 2019. Technology Green Synthesis : Photocatalytic Degradation of Textile Dyes Using Metal and Metal Oxide Nanoparticles-Latest Trends and Advancements Green Synthesis : *Crit. Rev. Environ. Sci. Technol*. 1-107.
76. Press, D. 2013. One-Step Green Synthesis and Characterization of Leaf Extract-Mediated Biocompatible Silver and Gold Nanoparticles from Memecylon Umbellatum. 1307-1315.
77. Liu, J. 2005. Scanning Transmission Electron Microscopy and Its Application to the Study of Nanoparticles and Nanoparticle Systems. 54: 251-278.
78. Ebelegi, A.N., N. Ayawei and D. Wankasi, D. 2020. Interpretation of Adsorption Thermodynamics and Kinetics. *Open Journal of Physical Chemistry* 10: 166-182.
79. Madian, H.R., A. E. Abdelhamid and H. M. Hassan, et al. 2024. Potential applicability of *Jatropha curcas* leaves in bioethanol production and their composites with polymer in wastewater treatment. *Biomass Conv. Bioref.* 14: 20991-21005.
80. Fito, J., S. Abrham and K. Angassa. 2020. Adsorption of methylene blue from textile industrial wastewater onto activated carbon of *parthenium hysterophorus*. *Int. J. Environ. Res.* 14 (5): 501-511.
81. Stabentheiner, E., A. Zankel and P. Polt. 2010. Environmental scanning electron microscopy (ESEM)-a versatile tool in studying plants. *Protoplasma* 246(1): 89-99.
82. Lagergren, S. 1898. About the theory of so-called adsorption of soluble substance. K. Sven. Vetersk. Handl. 24: 1-39.
83. Ho, Y.S and G. McKay. 1999. Pseudo-second order model for sorption processes. *Process Biochem*. 34: 451-465.
84. Langmuir, I. 1916. Constitution and fundamental properties of solids and liquids. I. Solids. *J. Am. Chem. Soc*. 38: 2221-2295.
85. Freundlich, H.M.F. 1906. Uber die adsorption in losungen. Z. *Phys. Chem*. 57: 385-470.

86. ICH Harmonised Tripartite Guideline. 2005. Validation of analytical procedures: text and methodology q2(r1). International conference on harmonization of technical requirements for registration of pharmaceuticals for human use 1-17.
87. Alfrhan, M.A., H. H. Hammud, M. A. Al-Omair and M. A. El-Sonbati. 2020. Uptake of crystal violet from water by modified Khalas dates residues. *Desalination Water Treat.* 174: 361-375.
88. Tesfaye Gari, M., B. Tessema Asfaw, S.K. Arumugasamy, L. Deso Abo and M. Jayakumar. 2023. Natural resources-based activated carbon synthesis, in: Encyclopedia of Green Materials. *Springer* 1-11.
89. Bejjanki, D., P. Banothu, V. B. Kumar and P. S. Kumar. 2023. Biomass-derived N-doped activated carbon from Eucalyptus leaves as an efficient super capacitor electrode material. *Chimia* 9(1): 24.
90. Yurtay, A and Kilic, M. 2023. Biomass-based activated carbon by flash heating as a novel preparation route and its application in high efficiency adsorption of metronidazole. *Diam. Relat. Mater*. 131: 109603.
91. Fito, J., et al. 2023. Adsorption of methylene blue from textile industrial wastewater using activated carbon developed from Rumex abyssinicus plant. *Sci. Rep*. 13(1): 5427.
92. Mengistu, A., M. Abewaa, E. Adino, E. Gizachew and J. Abdu, The application of *Rumex abyssinicus* based activated carbon for Brilliant Blue Reactive dye adsorption from aqueous solution. *BMC Chem.* 1-24.
93. Fito, J., et al. 2023. Journal of the Taiwan institute of chemical engineers adsorption of black MNN reactive dye from tannery wastewater using activated carbon of *Rumex abyssinicus*. *J. Taiwan Inst. Chem. Eng*. 151: 105138.
94. Yagub, M. T., T. K. Sen, S. Afroze and H. M. Ang. 2014. Dye and its removal from aqueous solution by adsorption. *Advances in Colloid and Interface Science* 209: 172-184.

7. APPENDIX

Appendix I: Pseudo first order origin output

Parameters

		Value	Standard Error	t-Value	Prob>|t|
ln qe-qt	Intercept	0.44085	0.24948	1.76708	0.12055
	Slope	-0.05078	0.00349	-14.53558	1.74058E-6

Slope is significantly different from zero (See ANOVA Table).

Standard Error was scaled with square root of reduced Chi-Sqr.

Statistics

	ln qe-qt
Number of Points	9
Degrees of Freedom	7
Residual Sum of Squares	1.15326
Pearson's r	-0.98384
R-Square (COD)	0.96793
Adj. R-Square	0.96335

Summary

	Intercept		Slope		Statistics
	Value	Standard Error	Value	Standard Error	Adj. R-Square
ln qe-qt	0.44085	0.24948	-0.05078	0.00349	0.96335

ANOVA

		DF	Sum of Squares	Mean Square	F Value	Prob>F
ln qe-qt	Model	1	34.80908	34.80908	211.28317	<0.0001
	Error	7	1.15326	0.16475		
	Total	8	35.96234			

At the 0.05 level, the slope is significantly different from zero.

Appendix II: Pseudo second order output

Parameters

		Value	Standard Error	t-Value	Prob>|t|
t/qt	Intercept	0.00491	0.00166	2.95955	0.02112
	Slope	0.02292	2.32147E-5	987.43563	2.88539E-19

Slope is significantly different from zero (See ANOVA Table).

Standard Error was scaled with square root of reduced Chi-Sqr.

Statistics

	t/qt
Number of Points	9
Degrees of Freedom	7
Residual Sum of Squares	5.0928E-5
Pearson's r	1
R-Square (COD)	0.99999
Adj. R-Square	0.99999

Summary

	Intercept		Slope		Statistics
	Value	Standard Error	Value	Standard Error	Adj. R-Square
t/qt	0.00491	0.00166	0.02292	2.32147E-5	0.99999

ANOVA

		DF	Sum of Squares	Mean Square	F Value	Prob>F
t/qt	Model	1	7.09375	7.09375	975029.12603	<0.0001
	Error	7	5.0928E-5	7.27543E-6		
	Total	8	7.09381			

At the 0.05 level, the slope is significantly different from zero.

Appendix III: Kinetic model parameters

Pseudo First Order						
Biosorbent	**Intercept**	**Slope**	**qe(mg/g)**	**K1 (min-1)**	**R^2**	**SSE**
	0.44085	**-0.05078**	**1.554027581**	**-0.000423167**	**0.96**	**1.15**

Pseudo Second Order							
Biosorbent	**Intercept**	**Slope**	**qe (mg/g)**	**qe2**	**K2 (g mg-1 min-1)**	**R^2**	**SSE**
	0.00491	**0.02292**	**43.63001745**	**1903.578423**	**0.10699112**	**0.99999**	**0.000051**

Appendix IV: Langmuir model output

Parameters

		Value	Standard Error	t-Value	Prob>|t|
1/qe	Intercept	-0.03006	0.01122	-2.67939	0.05526
	Slope	0.81249	0.05997	13.5489	1.71762E-4

Slope is significantly different from zero (See ANOVA Table).

Standard Error was scaled with square root of reduced Chi-Sqr.

Statistics

	1/qe
Number of Points	6
Degrees of Freedom	4
Residual Sum of Squares	0.00101
Pearson's r	0.98928
R-Square (COD)	0.97867
Adj. R-Square	0.97334

Summary

	Intercept		Slope		Statistics
	Value	Standard Error	Value	Standard Error	Adj. R-Square
1/qe	-0.03006	0.01122	0.81249	0.05997	0.97334

ANOVA

		DF	Sum of Squares	Mean Square	F Value	Prob>F
1/qe	Model	1	0.04633	0.04633	183.57258	1.71762E-4
	Error	4	0.00101	2.52371E-4		
	Total	5	0.04734			

At the 0.05 level, the slope is significantly different from zero.

Appendix V: Freundlich model output

Parameters

		Value	Standard Error	t-Value	Prob>|t|
Log qe	Intercept	0.05262	0.005	10.523	4.61199E-4
	Slope	0.68355	0.0052	266.1215	1.19616E-9

Slope is significantly different from zero (See ANOVA Table).

Standard Error was scaled with square root of reduced Chi-Sqr.

Statistics

	Log qe
Number of Points	6
Degrees of Freedom	4
Residual Sum of Squares	5.46319E-5
Pearson's r	0.99997
R-Square (COD)	0.99994
Adj. R-Square	0.99993

Summary

	Intercept		Slope		Statistics
	Value	Standard Error	Value	Standard Error	Adj. R-Square
Log qe	0.05262	0.005	0.68355	0.0052	0.99993

ANOVA

		DF	Sum of Squares	Mean Square	F Value	Prob>F
Log qe	Model	1	0.96727	0.96727	70820.65435	<0.0001
	Error	4	5.46319E-5	1.3658E-5		
	Total	5	0.96732			

At the 0.05 level, the slope is significantly different from zero.

Appendix VI: Adsorption model parameters

Langmuir						
Intercept	**Slope**	**q_{max} (mg/g)**	**K_L**	**R_L**	**R^2**	**MSE**
-0.03006	**0.81249**	**-33.26679973**	**-0.036997378**	**-1.17665204**	**0.97**	**0.00025**

Freundlich					
Intercept	**Slope**	**K_f**	**1/n**	**R^2**	**MSE**
0.05262	**0.68355**	**1.128807796**	**0.68355**	**0.99993**	**0.000055**

Appendix VII: Sample Collection

Appendix VIII: SEM analysis